Article

Cell Host & Microbe

Distinct Polysaccharide Utilization Determines Interspecies Competition between Intestinal *Prevotella* spp.

Graphical Abstract

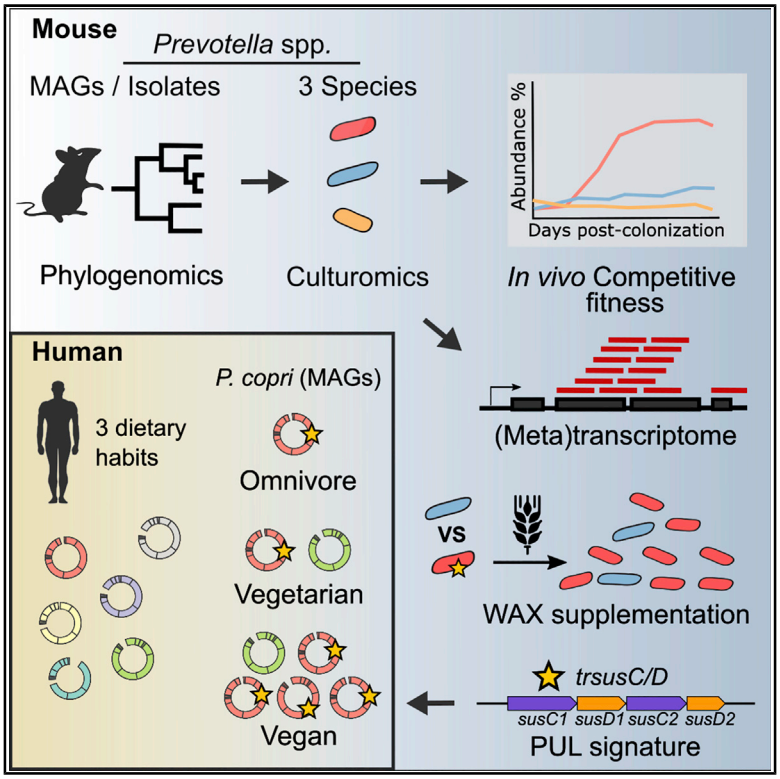

Highlights

- Metagenomics and culturomics characterization of *Prevotella* spp. in the mouse gut
- Distinct *Prevotella* spp. compete *in vivo* for similar plant-derived polysaccharides
- A dominant Prevotella strain encodes a specific PUL enabling arabinoxylan utilization
- Similar genetic features are found in human *Prevotella copri* strains enriched in vegans

Authors

Eric J.C. Gálvez, Aida Iljazovic, Lena Amend, ..., Achim Gronow, Emmanuelle Charpentier, Till Strowig

Correspondence

till.strowig@helmholtz-hzi.de

In Brief

Prevotella are among the most dominant bacteria found in the gut. Galvez et al. identify *Prevotella* species in the mouse gut and examine how one dominant species outcompetes commensal bacteria, including other *Prevotella* species, by encoding specific polysaccharide utilization loci (PULs), notably those enabling arabinoxylan utilization.

Gálvez et al., 2020, Cell Host & Microbe *28*, 838–852
December 9, 2020 © 2020 Elsevier Inc.
https://doi.org/10.1016/j.chom.2020.09.012

CellPress

CellPress

Cell Host & Microbe

Article

Distinct Polysaccharide Utilization Determines Interspecies Competition between Intestinal *Prevotella* spp.

Eric J.C. Gálvez,[1,2,3] Aida Iljazovic,[1] Lena Amend,[1] Till Robin Lesker,[1] Thibaud Renault,[3,4,5] Sophie Thiemann,[1] Lianxu Hao,[1] Urmi Roy,[1] Achim Gronow,[1] Emmanuelle Charpentier,[3,6] and Till Strowig[1,2,7,8,*]

[1]Department of Microbial Immune Regulation, Helmholtz Centre for Infection Research, Braunschweig, Germany
[2]Hannover Medical School, Hannover, Germany
[3]Max Planck Unit for the Science of Pathogens, Berlin, Germany
[4]CNRS/University of Bordeaux, UMR 5234, Microbiologie Fondamentale et Pathogénicité, France
[5]Institut Européen de Chimie et Biologie, Université de Bordeaux, Pessac, France
[6]Institute for Biology, Humboldt University, Berlin, Germany
[7]Centre for Individualized Infection Medicine, Hannover, Germany
[8]Lead Contact
*Correspondence: till.strowig@helmholtz-hzi.de
https://doi.org/10.1016/j.chom.2020.09.012

SUMMARY

Prevotella spp. are a dominant bacterial genus within the human gut. Multiple *Prevotella* spp. co-exist in some individuals, particularly those consuming plant-based diets. Additionally, *Prevotella* spp. exhibit variability in the utilization of diverse complex carbohydrates. To investigate the relationship between *Prevotella* competition and diet, we isolated *Prevotella* species from the mouse gut, analyzed their genomes and transcriptomes *in vivo*, and performed competition experiments between species in mice. Diverse dominant *Prevotella* species compete for similar metabolic niches *in vivo*, which is linked to the upregulation of specific polysaccharide utilization loci (PULs). Complex plant-derived polysaccharides are required for *Prevotella* spp. expansion, with arabinoxylans having a prominent impact on species abundance. The most dominant *Prevotella* species encodes a specific tandem-repeat *trsusC/D* PUL that enables arabinoxylan utilization and is conserved in human *Prevotella copri* strains, particularly among those consuming a vegan diet. These findings suggest that efficient (arabino)xylan-utilization is a factor contributing to *Prevotella* dominance.

INTRODUCTION

The gut microbiota fulfills diverse functions for the host, including the degradation of dietary complex polysaccharides, thereby, releasing nutrients and metabolites that can be utilized by the host. The gut microbiota of adults is typically dominated by bacterial species belonging to the phylum Bacteroidetes and Firmicutes, while members of the phylum Proteobacteria, Actinobacteria, Verrucomicrobia, and Fusobacteria are found in lower abundances (Human Microbiome Project Consortium, 2012). Within Bacteroidetes, members of the genus *Prevotella* have emerged as underexplored keystone species not only within the human microbiome but also in many animal microbiomes. In the human gut, *Prevotella copri* represents the most abundant species followed by *Prevotella stercorea* (Hayashi et al., 2007; Li et al., 2009). Enhanced *Prevotella* spp. prevalence was identified in non-Westerners as well as individuals consuming a plant-rich diet (Clemente et al., 2015; Martínez et al., 2015; Tett et al., 2019). The presence of *P. copri* has been linked to improved glucose metabolism after intake of specific prebiotics (Kovatcheva-Datchary et al., 2015). Together, these studies suggest that *Prevotella* is an ancient and potentially beneficial commensal. Conversely, other studies have associated *Prevotella* spp. with inflammatory diseases in humans and mice (Dillon et al., 2014; Elinav et al., 2011; Wen et al., 2017). Specifically, an overabundance of *P. copri* or the genus *Prevotella* was associated with increased risk for rheumatoid arthritis (Alpizar-Rodriguez et al., 2019; Scher et al., 2013; Wells et al., 2019). This divergent modulation of the host physiology by the *Prevotella* spp., particularly *P. copri*, may be caused by multiple factors, e.g., distinct species and strains differing in their functional and metabolic capabilities. Indeed, metagenomic studies of *P. copri* have unveiled a high intraspecies diversity as evidenced by at least four genetically distinct clades and co-presence of multiple clades has been detected predominantly in individuals from non-Westernized countries (Tett et al., 2019). Moreover, genomic characterization of, for e.g., carbohydrate utilization has identified extensive variability in the ability to utilize diverse complex carbohydrates in *P. copri* strains (Fehlner-Peach et al., 2019). Yet, a shared property between *P. copri* strains was predicted to be the ability to degrade xylan, which is the major component of many plant-cell walls. Besides *P. copri*, the potential to degrade various

structurally related xylan forms has been found in various intestinal Bacteroidetes. For instance, the human gut commensal *Bacteroides ovatus* as well as *Prevotella bryantii* and *Prevotella ruminicola*, both found in the rumen of cows, encode highly conserved clusters of starch utilization systems (*Sus*) that are highly induced during *in vitro* growth on arabinoxylans (Dodd et al., 2010, 2011; Martens et al., 2011; Rogowski et al., 2015). Notably, these arabinoxylan-utilizing *Sus*-like elements have a particular organization compared with other PULs containing tandem-repeat *SusC* and *SusD* proteins (*trSusC/D*), which are rare and approximately represent only around 3% of the encoded PULs in the phylum Bacteroidetes (Lapébie et al., 2019). Supporting the role of plant-derived polysaccharides for *Prevotella* spp. expansion is the reproducibly observed increase of *Prevotella* OTUs after plant-polysaccharide diet interventions, as determined using the 16S rRNA gene marker surveys (Chen et al., 2017; David et al., 2014; Kovatcheva-Datchary et al., 2015; Wu et al., 2011). However, the preferred glycan substrates and the *in vivo* functional responses to diet interventions have not been explored in detail in *P. copri* or other *Prevotella* spp., partly due to the lack of isolates for versatile animal models such as the mouse. Moreover, it remains unclear how related *Prevotella* strains and species potentially co-operate or compete for specific nutrients and how *Prevotella* spp. outcompete other commensals as they are frequently the most abundant bacteria in fecal samples.

RESULTS

Distinct *Prevotella* Strains Govern the Mouse Gut Microbiome

Multiple distinct operational taxonomic units (OTUs) belonging to uncultured species of the genus *Prevotella* have been previously identified in mice (Gálvez et al., 2017). To comprehensively characterize the diversity of intestinal *Prevotella* spp. in mice, we screened the intestinal microbiota composition of twelve laboratory mouse lines obtained from four commercial breeders as well as our research institute using 16S rRNA gene sequencing (Figure 1A; Table S1). In line with previous reports, beta-diversity analysis demonstrated that the mouse gut microbiota composition is strongly influenced by the originating breeding facility (ADONIS, $R^2 = 0.41$, p value < 1e-04), while barrier had a smaller effect within the tested vendors (Figure S1A). Of note, the *Prevotella* to *Bacteroidales* ratio (abundance of *Prevotella*/sum [*Bacteroidales*]) revealed an abundance gradient that correlates with each vendor's cluster, demonstrating a significant influence of the abundance of the genus *Prevotella* on the overall community structure similar to human enterotypes (Figure S1B) (Costea et al., 2017; Gorvitovskaia et al., 2016). Analysis of members of the *Prevotella* genus at the OTU level (USEARCH, similarity 97% within V4 region, abundance > 0.2%), revealed 5 distinct *Prevotella* OTUs in the gut community, either being present alone or in combination with another *Prevotella* OTU (Figure 1B; Table S1). Of all detected *Prevotella* phylotypes, OTU_1 was the most prevalent being present in multiple vendors, while OTU_12 and OTU_16 were highly abundant but only in specific mouse lines (Table S1). Phylogenetic analysis showed that *Prevotella* OTUs are grouped in three main lineages and the large sequence distance between groups suggested that each OTU could be associated with distinct species (Figure S1C).

To complement the 16S rRNA gene-based studies, a recent resource was mined, the integrated mouse gut metagenome catalog (iMGMC), that comprises a collection of 20,927 metagenome-assembled genomes (MAGs) (quality MAG: completeness $\geq$ 50%, contamination < 10%) recovered from the metagenome sequencing of 871 laboratory and wild mouse samples (Lesker et al., 2020). Of these MAGs, a set of 252 MAGs was identified to be members of the genus *Prevotella* (GTDB-Tk taxonomic assignments, see STAR Methods for details) (Figure 1C). Phylogenetic comparison with reference genomes of the genus *Prevotella* and *Paraprevotella* confirmed 5 species clusters (Figure 1D). Of note, MAGs did not differ in their quality between clusters (Figures S1D and S1E) and MAGs from 2 of the 5 species (clusters 1 and 4) were recovered from the gut microbiome of both laboratory and wild mice demonstrating that *Prevotella* spp. are natural commensals of the gut ecosystem, similar to the microbiota of humans and other animals (Figure 1D).

Guided by the identification of distinct OTUs or species clusters in specific mouse lines, we utilized a stepwise enrichment and isolation scheme under strictly anaerobic conditions to isolate representatives of these previously undescribed *Prevotella* spp. (see STAR Methods for details). This cultivation effort initially yielded seven distinct bacterial strains representing the five *Prevotella* clusters based on the comparison of their genomes and 16S rRNA genes with the clusters and other described *Prevotella* species (Figures 1D and S1C; Table S1), respectively. Unfortunately, isolates from two species failed to be recovered after cryoconservation. The other three previously undescribed species *Prevotella sp. nov. strain* PROD (referred to as *Prevotella rodentium*, DSM103721: OTU_1, cluster 5), *Prevotella sp. nov. strain* PINT (referred to as *Prevotella intestinalis*, DSM103738; OTU_16, cluster 1), and *Prevotella sp. nov. strain* PMUR (referred to as *Prevotella muris*, DSM103722, OTU_12, cluster 3) could be recovered after cryoconservation and were deposited in a public repository.

Together, these data uncover an underappreciated diversity of *Prevotella* spp. in the mouse gut identifying 5 different clusters for which 3 representative isolates are now publicly available for functional *in vivo* studies.

Competition Dominates Interactions among *Prevotella* spp.

Diverse *Prevotella* spp. can co-exist in variable abundance in the intestine of mice and humans presumably filling distinct and overlapping metabolic niches (Fehlner-Peach et al., 2019; Tett et al., 2019). With the aim to investigate the ecological interactions among *Prevotella* species in mice, we performed a microbiome competition experiment by indirectly mixing the most prevalent and abundant species (clusters 1, 3, 4, and 5) followed by quantification of the colonization dynamics. Therefore, five different mouse lines were cohoused: three mouse lines harboring strains from distinct *Prevotella* species, (*P. intestinalis* and OTU_15 in CONV_N6 (*Nlrp6*$^{-/-}$), *P. rodentium* in SPF_jan (*wt*), and *P. muris* in SPF_nci (*wt*) with two mouse lines lacking members of *Prevotella* spp., i.e., SPF_hzi (wt) (Iljazovic et al., 2020; Lesker et al., 2020) and a germ-free mouse strain (exGF Swiss Webster) (Figure 2A). Five mice, i.e., one of each mouse line, were co-

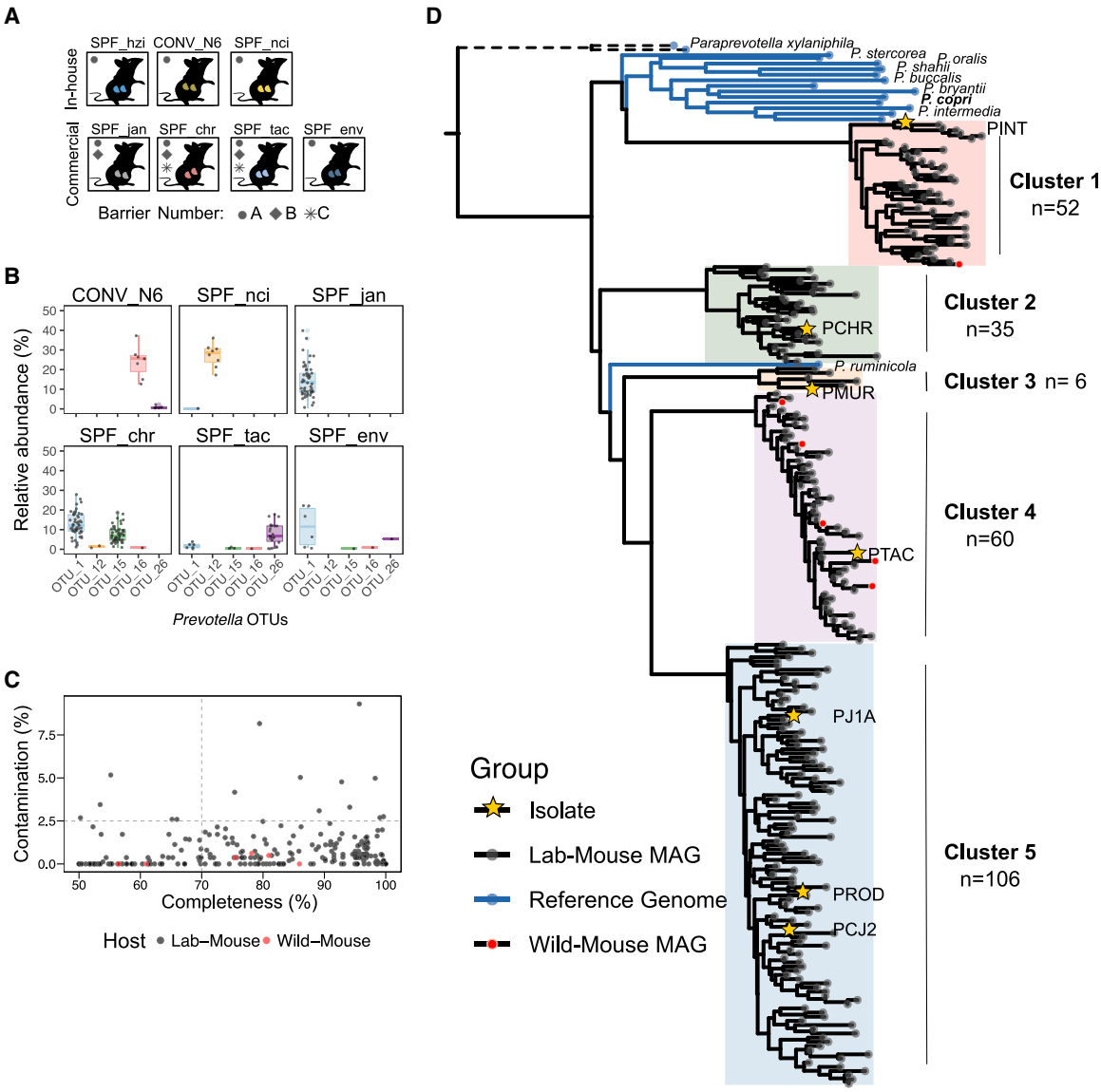

Figure 1. Previously Uncharacterized *Prevotella* Species Dominate the Mouse Gut Microbiome

(A) Overview of surveyed mouse-breeding facilities. Boxes indicate facilities (in-house) or vendors (commercial), respectively; inner shapes indicate the number of screened barriers (n = 2–3 hygiene barriers per breeder; 9–44 mice per barrier).

(B) Dominance of distinct *Prevotella* OTUs in mouse lines; x axis indicates *Prevotella* OTUs (USEARCH_v8.1, > 97% similarity) and y axis indicates relative abundance (%).

(C) Quality assessment of all 252 reconstructed mouse *Prevotella* MAGs (iMGMC, Lesker et al., 2020). Black dots represent MAGs assembled from laboratory mice and red dots represent MAGs reconstructed from wild-mice samples.

(D) Genome-based phylogenetic tree of mouse *Prevotella* isolates clustered with 259 metagenome-assembled genomes (MAGs) of the genus *Prevotella* from the mouse gut metagenome catalog (Lesker et al., 2020) and reference genomes of the genus *Prevotella*. Black branches represent MAGs associated with laboratory mice (black dots). MAGs reconstructed from wild-mice samples are highlighted with red dots. Stars represent each of the seven isolated strains. *Paraprevotella xylaniphila* and *Paraprevotella clara* were used as outgroups (clade in dotted line). The phylogeny was inferred using 400 universal bacterial maker gene sequences (PhyloPhlan2, see STAR Methods).

See also Figure S1; Table S1.

housed together in a cage for 21 days, and this setup was replicated four times. Fecal pellets were collected before co-housing as well as after 7 and 21 days of co-housing. Microbiota composition was analyzed using 16S rRNA gene sequencing. Ordination analysis considering the variables "microbiota" and "timepoint" showed distinct and reproducible colonization dynamics over time (Figure 2B). As expected, samples before co-housing (day −1) clustered by mouse line. After 7 days of co-housing two different colonization patterns emerged, the exGF and SPF_nci mice resembled the CONV_N6 microbiota, while the SPF_hzi samples were more similar to the SPF_jan mice. Strikingly, after 21 days of co-housing all samples converged in one cluster close

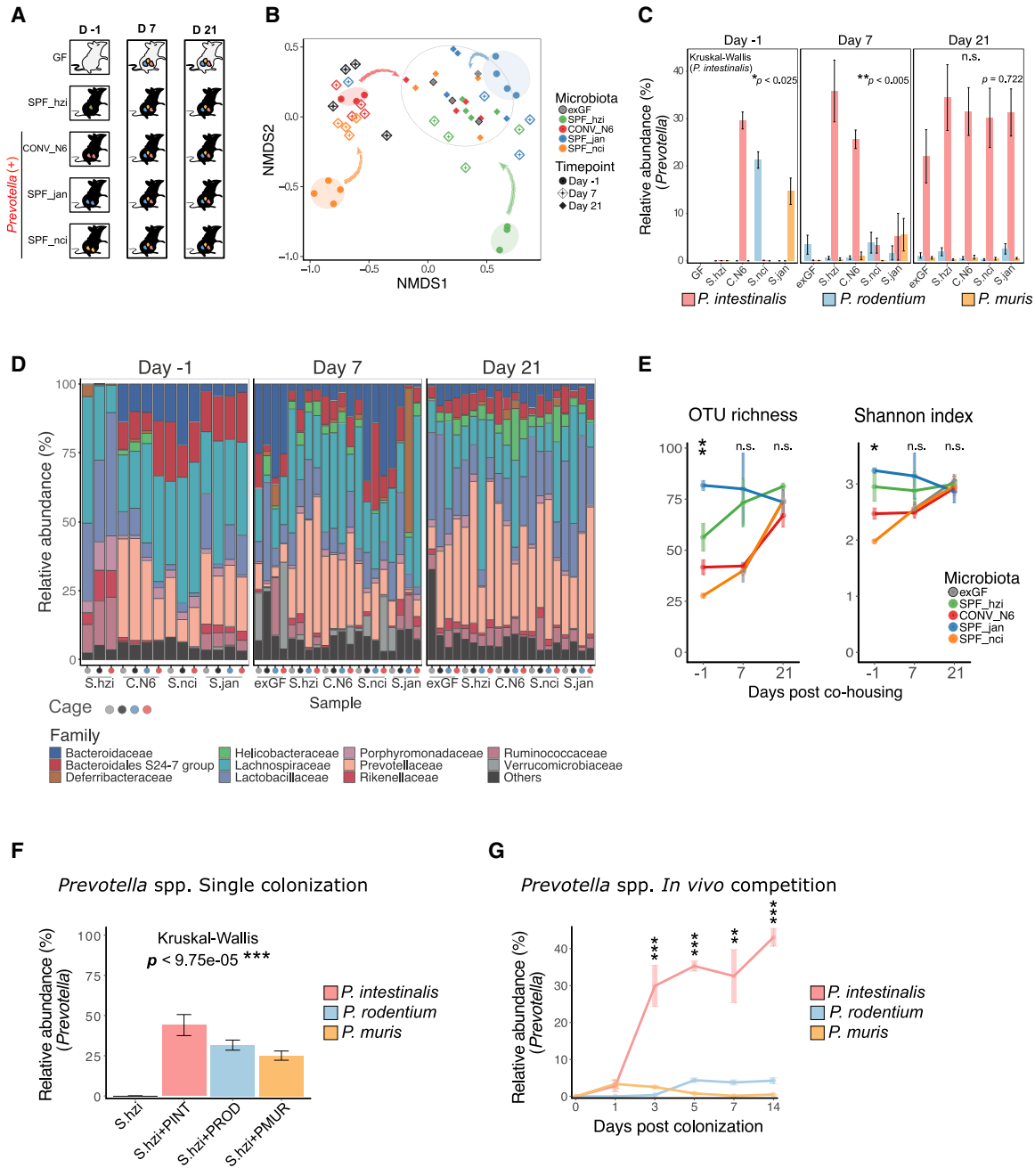

Figure 2. *Prevotella intestinalis* Outcompetes Other *Prevotella* spp. in the Mouse Gut

(A–E) Cohousing of mouse lines and longitudinal analysis of microbiota composition using 16S rRNA gene sequencing.

(A) Scheme of experimental design for *Prevotella*-microbiome competition.

(B) NMDS ordination analysis (Bray-Curtis distances) of microbiota composition before (day −1) and during cohousing (day 7 and day 21). Colors denote the mouse lines, shapes indicate time points.

(C) Relative abundance (%) of *P. intestinalis*, *P. rodentium*, and *P. muris*. Bars represent mean values for each mouse colony before (day −1) and during cohousing (day 7 and day 21). Error bars show ± SEM, n = 3–4 animals per breeder. Differences in relative abundance of *P. intestinalis* were tested for each time point *p < 0.05 (Kruskal-Wallis test).

(D) Taxonomic bar plots of the 15 most abundant families in individual samples before and after co-housing. Labels on the bottom indicate the mice breeder and colored dots represent cages (n = 5 mice per cage; cages n = 4).

(E) Quantification of α-diversity using observed species richness and Shannon index. Mean values ± SEM (vertical shading) are indicated, n = 3–4 animals/treatment. *p < 0.05 (Kruskal-Wallis test).

(legend continued on next page)

to but distinct from the initial SPF_jan microbiota suggesting that the ecosystem then reached a new stable state. Next, we wanted to identify whether the co-housing resulted in the co-presence of *Prevotella* species or rather in competition and dominance by a single species. Initially, overexpansion of the species *P. intestinalis* was noted after 7 days of co-housing only in SPF_hzi mice reaching up to 35.8% of mean relative abundance (Figure 2C; Table S2). The second most abundant *Prevotella* species in the first week of co-housing was *P. rodentium*, which interestingly rapidly colonized the exGF mice. *P. muris* displayed the lowest colonization, and its relative abundance dropped from 14.6%, before co-housing, to 5.5% at day 7 in SPF_nci mice. Strikingly, after 21 days *P. intestinalis* outcompeted *P. rodentium* and *P. muris* reaching in all mouse lines a high relative abundance (29.8%) in contrast with *P. rodentium* (1.3%) and *P. muris* (0.5%). The additional OTU_15 initially present in CONV_N6 was under the detection limit. While this suggests that these distinct *Prevotella* spp. strains compete with each other for a metabolic niche, taxonomic analysis on the family level revealed additional changes in the community after the co-housing, e.g., the increased prevalence of Lactobacillaceae, Muribaculaceae, and Helicobacteriaceae (Figure 2D). Similarly, alpha diversity analysis showed an increase in all mouse lines except the SPF_jan mouse line, which had the highest alpha diversity before the co-housing (Figure 2E). Thus, the dominance of *P. intestinalis* from CONV_N6 mice in this experiment is associated with changes in taxonomic composition and diversity, and it may not result from direct competition between *Prevotella* spp. Therefore, we next performed additional colonization experiments in a standardized *Prevotella*-free host (Iljazovic et al., 2020; Lesker et al., 2020). We first assessed the colonization potential of each individual *Prevotella* strain, and all three tested *Prevotella* strains reached in SPF_hzi mice a mean relative abundance of 33.5% (SEM ± 5.6%) after 14 days (Figure 2F) demonstrating that each species individually is able to efficiently colonize this mouse line. Next, competitive colonization was performed by mixing the three *Prevotella* species before introducing them into SPF_hzi recipient mice. Longitudinal 16S rRNA gene analysis revealed that *Prevotella* spp. were stably detectable already after 3 days and that, strikingly, *P. intestinalis* DSM103738 outcompeted the other two species (43.0%, SEM ± 2.4% versus 4.3% versus 0.5% at day 14) (Figure 2G). Together, these results indicate that *Prevotella* species strongly compete in the mouse gut suggesting that genome diversity does not reflect complementary metabolic functions for cooperation as observed in some species of Bacteroides (Rakoff-Nahoum et al., 2016).

Presence of Distinct Glycoside Hydrolases (GHs) and Putative Polysaccharide Utilization Loci (PULs) Correlate with High Fitness in *P. intestinalis*

Dietary polysaccharides are recognized as major factors in shaping the composition and physiology of the gut microbiome (Koropatkin et al., 2012). To characterize the carbohydrate degradation potential in the *Prevotella* clusters, we predicted carbohydrate-active enzymes (CAZymes) in the isolated strains and *Prevotella* MAGs using a bioinformatic approach (dbCAN2 tool; Zhang et al., 2018). To avoid any bias due to low completeness and high contamination we restricted the analysis to 168 *Prevotella* spp. MAGs with a completeness of >70% and contamination < 2.5% (Figure 1C). The prediction unveiled that *P. intestinalis*/cluster 1, *P. rodentium*/cluster 5, and *P. muris*/cluster3 (162 CAZymes) encoded higher numbers of features compared with the other two clusters (Figure 3A). Notably, clustering of MAGs and isolates based on their CAZyme profiles revealed that each species complex except cluster 3, which contained the fewest genomes, formed a distinct cluster (Figure S2A) (Lombard et al., 2014). The most abundant enzyme classes were the carbohydrate-degrading GHs and glycosyltransferases (GTs) (Figure S2B; Table S3). GHs are a complex and widespread group of enzymes, which degrade polysaccharides by catalyzing the hydrolysis and/or rearrangement of glycosidic bonds. Classification according to GHs families showed that GH43, GH2, and GH28 are the most abundant CAZymes in *Prevotella* isolates and MAGs. The GH43 family contains endoxylanases, β-xylosidases, and α-L-arabinofuranosidases, which may play a key role in the de-branching and cleavage of xylans, while the GH2 family in bacteria has been commonly associated with β-galactosidases and β-glucuronidase activity. The GH28 family is commonly active against rhamnogalacturonan, which forms the branched part of the pectin molecule. Comparative analysis of GHs families in isolates revealed that *P. intestinalis* DSM103738 contains a set of 7 GHs, which are absent in *P. rodentium* DSM103721 and *P. muris* DSM1037212 (Figure 3B). The group of GH enzymes comprehends β-l-arabinofuranosidase (GH137), α-galacturonidase (GH138), α-2-O-methyl-l-fucosidase (GH139), α-l-fucosidase (GH141), DHA-hydrolase (GH143), α-L-rhamnosidase (GH145), and a complex of chitinases, lysozyme, and xylanase inhibitors (GH18) (Figure 3B). Interestingly, GH137, GH138, GH139, GH141, and GH143 belong to the recently described rhamnogalacturonan-II (RG-II) degradome, one of the most complex glycan currently known (Ndeh et al., 2017). Other GH enzymes were specific to *P. rodentium* and *P. muris* (Figure 3B).

CAZymes are in bacteria often part of larger gene units known as PULs (Bjursell et al., 2006). Prediction of PULs based on *susC*/*susD*-like pairs using PULpy (Stewart et al., 2018) identified the highest number of PULs in *P. intestinalis*/cluster 1 and cluster 2, while lower numbers of PULs were identified in *P. rodentium*/*cluster 5*, *P. muris*/*cluster 3*, and cluster 4 (Figure 3A; Table S4).

In order to analyze which of the CAZymes and PULs are utilized for growth *in vitro* and *in vivo*, global gene expression analysis was performed (Figures 3C–3E). Specifically, we

(F) SPF_hzi mice were colonized with individual *Prevotella* strains and microbiota composition was analyzed in fecal samples after 4 weeks of colonization using 16S rRNA gene sequencing. Bars show mean relative abundance (%) of each *Prevotella* strain. Error bars show ± SEM. n = 8 animals per strain. ***$p < 0.001$ (Kruskal-Wallis test).

(G) SPF_hzi mice were colonized with a mixture of three *Prevotella* strains and microbiota composition was analyzed in fecal samples longitudinal at indicated time points using 16S rRNA gene sequencing. Mean values ± SEM are indicated, n = 5 animals per strain. *$p < 0.05$ (Kruskal-Wallis test).

See also Table S2.

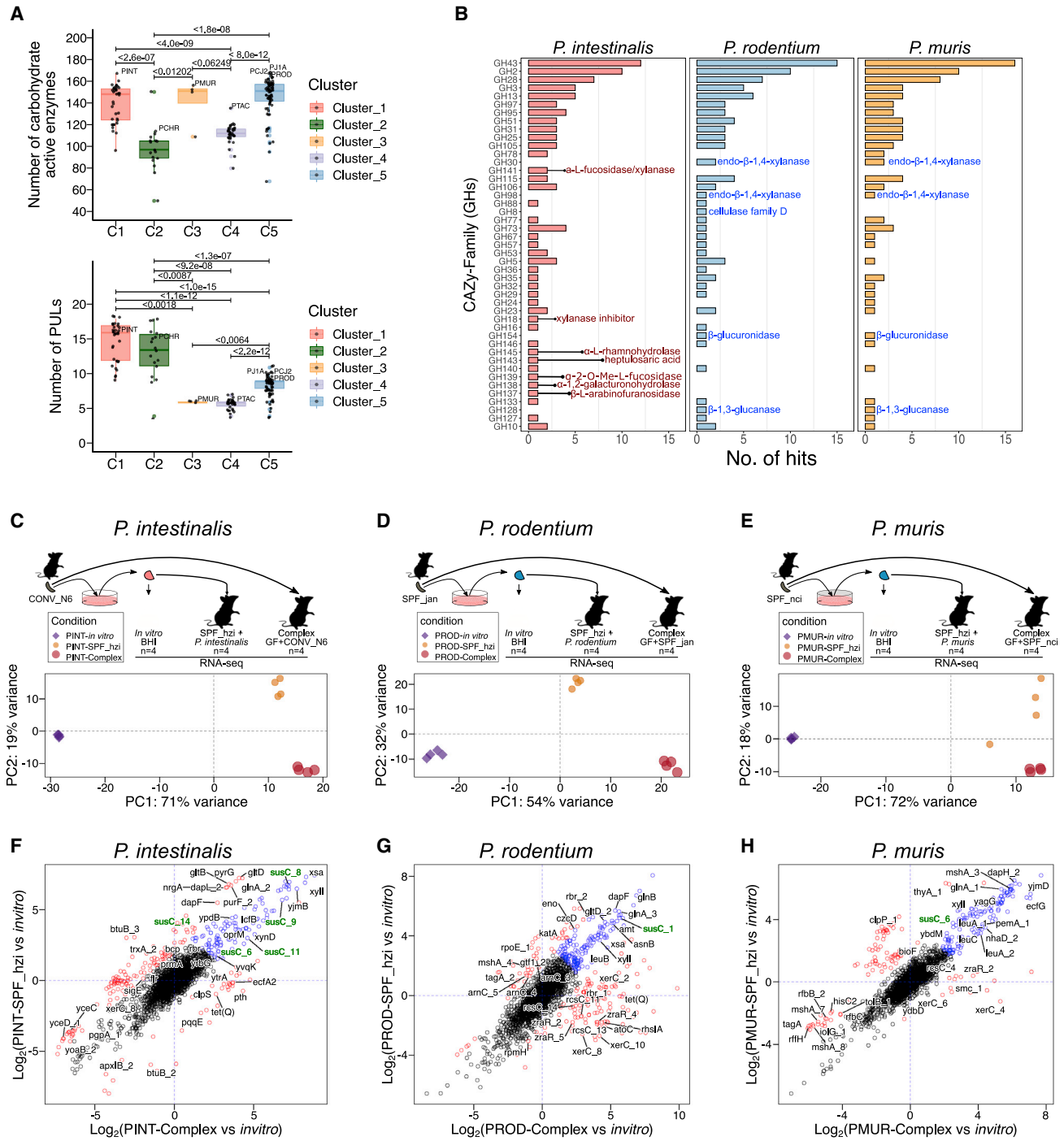

Figure 3. Diversity of Carbohydrate-Active Enzymes (CAZymes) in *Prevotella ssp* and *In Vivo* Expression of Starch Utilization Systems (*sus*)

(A) Genome-wide prediction of total carbohydrate-active enzymes modules (CAZymes) and polysaccharide utilization loci (PULs) in each mouse *Prevotella* cluster (MAGs n = 151, isolates n = 7). *p < 0.05 (Mann-Whitney U test).

(B) Presence or absence of GHs families in *P. intestinalis* DSM103738, *P. rodentium* DSM103721, and *P. muris* DSM103722. Differentially encoded GHs are listed.

(C–H) Characterization of murine *Prevotella* spp. transcriptome using RNA-seq.

(C–E) Experimental design and principal component analysis (PCA plot) of the gene expression (normalized RNA-seq counts, see STAR Methods) in *P. intestinalis* (C), *P. rodentium* (D), and *P. muris* (E). Transcriptome was compared between isolates ("*in vitro*") and *in vivo* after colonization of SPF_hzi mice ("SPF_hzi") with isolates or after transfer of indicated complex microbiomes, i.e., the origins of the isolates, into GF mice ("complex"). Data are representative of 4 biological replicates.

(F–H) Differential gene expression in *Prevotella* spp. (log_2 fold-change between complex microbiome and SPF_hzi), where fold-change (FC) in x axis corresponds to the difference between "complex-microbiome" and "*in vitro*"; while the y axis corresponds to "SPF_hzi" versus "*in vitro,*" respectively. The genes that

(legend continued on next page)

compared gene expression profiles during growth *in vitro* and *in vivo*. For the *in vivo* analysis, two groups were included: (1) SPF_hzi mice colonized with *Prevotella* isolate strains individually, and (2) the original mouse line from where each *Prevotella* species was isolated (referred to as complex) (see STAR Methods for details). Principal component analyses (PCA) revealed distinct transcriptional landscapes for each strain between *in vitro* and *in vivo* conditions (Figures 3C–3E). Interestingly, unexpected large variations in gene expression were observed between the two *in vivo* microbiota communities for each strain demonstrating the impact of distinct microbial interactions on shaping the transcriptional profile in *Prevotella* species (Figure S3; Table S5). To investigate the *in vivo* metabolic niche of each strain, independent pair-wise comparisons between the *in vitro* conditions versus the two *in vivo* conditions were performed using the DESeq2 package (log_2 fold change >2; p adj value < 0.01) (Figures 3F–3H). Of note, for each of the comparisons, approximately one-third of the genes (mean 863 features) was differentially expressed (Figure S3; Table S5). Using log_2-to-log_2 fold change analysis, a set of commonly overexpressed genes *in vivo* involved in the degradation of complex polysaccharides and nitrogen fixation was identified for all *Prevotella* spp. (Figures 3F–3H, upper right quadrant, Table S5). Specifically, we found several enzymes associated with arabinoxylan degradation, such as *xylI* (Endo-1, 4-beta-xylanase A) *xsa* (Xylosidase/arabinosidase), *xynD* (Arabinoxylan arabinofuranohydrolase), and a group of genes analogous to starch utilization systems (*sus*). Notably, five *susC* genes were highly upregulated in *P. intestinalis* in both microbiomes *in vivo*, while only a single *susC* gene was each upregulated *in vivo* in *P. rodentium* and *P. muris* (Figures 3F–3H). Identification of the most expressed PULs *in vivo* revealed that *P. intestinalis* utilizes four main PULs *in vivo* (PUL8, PUL10, PUL11, and PUL12), which notably are absent in *P. rodentium* and *P. muris* (Figures 4A–4C and S2; Table S5). Based on the CAZymes' trophic guilds (Accetto and Avguštin, 2015) within each PUL, we predicted the potential substrates for each of them (Figures 4A–4C). This analysis indicates that PUL10 of *P. intestinalis* is potentially involved in pectin degradation (comprises 3 copies of PL1), while PUL11 is predicted to degrade xylans (2× GH10, 2× GH43). The PUL8 and PUL12 did not include known CAZymes, and it was, therefore, not possible to infer the trophic guild. Of note, PUL11 and PUL8 contained tandem repeat *susC*/*susD* pairs (*trsusC*/*D*), which have been previously associated with (arabino)xylan catabolism and are found in some *P. copri* strains (Fehlner-Peach et al., 2019; Rogowski et al., 2015) (Figures 4A and S2B). Similar trsusC/D pairs were found 23 of 58 MAGs from the *P. intestinalis*/cluster1 (Figure S2C). Strikingly, while *P. muris* and *P. rodentium* encoded related GHs and PLs, the genome of none of the isolates and MAGs from cluster 2 to 5 including *P. muris* and *P. rodentium* contained any *trsusC*/*D* elements (Figure S2C). Together, the genome analysis with CAZyme prediction and PULs reconstruction as well as transcriptome analysis suggests that *P. intestinalis* encodes and expresses distinct putative xylan- and pectin-degrading gene clusters, which could provide *P. intestinalis* a competitive advantage over other bacteria, including outcompeting *Prevotella* species, in the presence of specific complex carbohydrates.

Diet Rich in Arabinoxylans Modulates the Abundance of Dominant *Prevotella* spp. in the Mouse Gut

In order to investigate whether complex plant-based polysaccharides are required for *P. intestinalis* domination in the large intestine, we performed an *in vivo* diet intervention in SPF_hzi mice additionally colonized with the two dominant *Prevotella* strains, *P. intestinalis* DSM103738 and *P. rodentium* DSM103721, which previously were identified to coexist with an advantage for *P. intestinalis* (see Figure 2G). Initially, mice were kept on a standard chow diet rich in complex plant-based polysaccharides (Stand-PP) and, subsequently, they were divided into three different groups: a control group maintained with Stand-PP and two experimental groups fed for 7 days one of two semisynthetic diets containing only starch and cellulose as polysaccharide. The two diets differed in their content of fat and simple sugars (Synth-HF: high fat, low sugar; Synth-LF: normal fat, high sugars) to mimic different types of Westernized diets. Finally, both experimental groups were returned to regular chow (Stand-PP) (Figure 5A). After *Prevotella* colonization, the control group (Stand-PP) remained stable during the experiment, while the other groups exhibited consistent diet-induced changes in the microbiota (Figure 5B; day 1 to day 7). Analysis of the microbiome composition at the level of family unveiled distinct response patterns. After colonization with *P. intestinalis* and *P. rodentium*, a reduction of Rikenellaceae and Lachnospiraceae was observed (Figure 5C, day −14 versus day −1). Switching the mice to semisynthetic diets (day −1 versus day 1) reduced the abundance of Prevotellaceae 12.6-fold in Synth-HF (from 57.2%, SEM ± 7.6% to 4.1%, SEM 1.1%) and 3.4-fold in Synth-LF (from 39.4%, SEM ± 5.5% to 9.0%, SEM ± 2.7%), while the relative abundances of Ruminococcaceae and Porphyromonadaceae increased (Figure 5C). A detailed analysis of the relative abundance of the *Prevotella* species showed an initial dominance of *P. intestinalis* over *P. rodentium*, as previously observed (Figure 5D). Diet intervention dramatically reduced the abundance of both *P. intestinalis* (Synth-HF: 45.1% SEM ± 5.4, to 3.3% SEM ± 1.0; Synth-LF: 30.0% SEM ± 3.6% to 7.6% SEM ± 2.5%) and *P. rodentium* (Synth-HF: 11.1% SEM ± 2.3% to 0.8% SEM ± 0.1; Synth-LF: 9.4% SEM ± 2.2% to 1.4% SEM ± 0.2%) (Figure 5D). Of note, returning the mice to Stand-PP diet rapidly increased the relative abundance of both *Prevotella* species within 1 day of diet switch (Figure 5D). To investigate whether this behavior is microbiota-context dependent, a similar experiment was performed using SPF_hzi mice that received the complex microbiota of CONV_N6 and SPF_jan mice. After fecal microbiota transplantation (FMT),

commonly upregulated in "complex-microbiome" as well as in "SPF_hzi" are represented in blue, genes with a differentially expression (FC > 2, p adj < 0.01) in one of the *in vivo* conditions are highlighted in red. Labeled genes indicated genes with a known function. Differentially expressed *susC* genes are highlighted in green. *P. intestinalis* (F), *P. rodentium* (G), and *P. muris* (H).
See also Figure S2; Table S3.

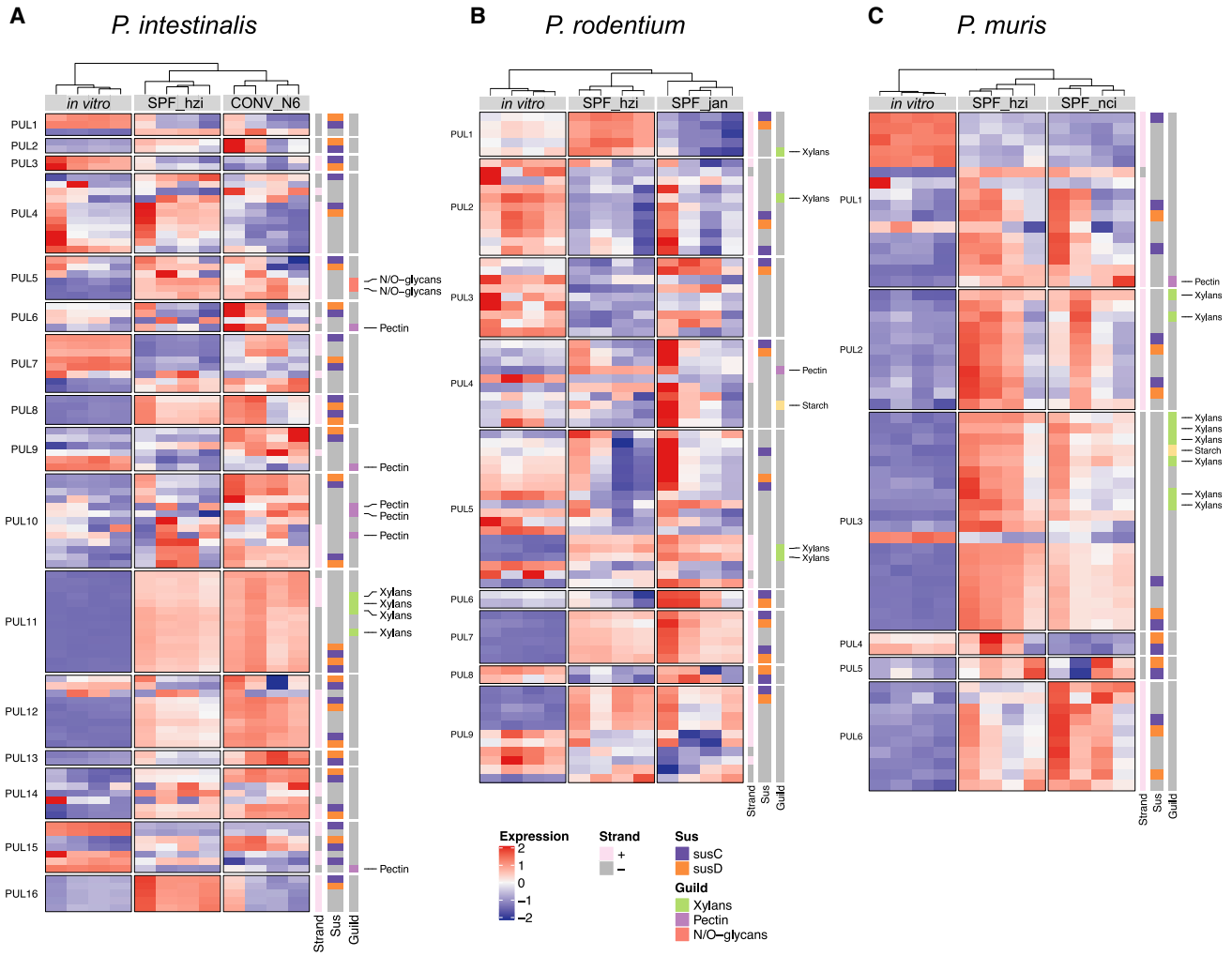

Figure 4. *In Vivo* Expression of *Polysaccharide* Utilization Loci (PUL) in *Prevotella* spp.

(A–C) Transcriptome analysis of PULs in *Prevotella* spp. Prediction resulted in 16 loci for (A) *P. intestinalis*, (B) 9 loci for *P. rodentium*, and (C) 6 for *P. muris*. Heatmaps represent normalized read counts (row-wise scaled) for each *Prevotella* spp. transcriptome. Right columns on each heatmap denote the coding strand of each feature, the location of the starch utilization systems (*susC* in purple and *susD* in orange) genes, and the trophic guild based on adjoining CAZymes. Data are representative of 4 biological replicates.

See also Figure S3; Tables S4 and S5.

mice harbored a more diverse community containing additional species, for instance from the order Bacteroidales (S24-7, Bacteroidaceae) and the phyla Proteobacteria (*Desulfovibrio* and *Helicobacter*) (Figure S4C). Similarly, *P. intestinalis* dominated the gut of mice fed with a standard chow diet but decreased dramatically after the shift to the semi-synthetic diet (Figure S4D). In turn, an over-expansion of Bacteroidales (S24-7 and Bacteroidaceae), as well as Ruminococcaceae in Synth-HF and Synth-LF, was observed. This indicates that in different microbiota settings, *Prevotella* spp. dominate the gut in the presence of complex plant-derived polysaccharides but are rapidly outcompeted in Westernized diets.

To identify which complex carbohydrates enable *Prevotella* spp. expansion, SPF_hzi mice were colonized with the isolates *P. intestinalis* and *P. rodentium* on chow diet (Stand-PP) and subsequently switched to Synth-LF diet for 4 days (Figure 5E). Then, mice were divided into different groups receiving either no additional carbohydrates, wheat arabinoxylan (WAX), pectin, or cellulose (as a control) in the drinking water (10 g/l). As expected feeding the mice with Synth-LF diet rapidly altered the microbiota, while WAX feeding resulted in a shift in the microbial community toward the microbiota composition on chow diet (Stand-PP) (Figure 5F). This shift could be explained by an increased relative abundance of *Prevotella* spp. in WAX-fed mice compared with mice fed no additional polysaccharide or those being fed pectin and cellulose (Figure 5G). Strikingly, WAX-supplementation resulted in the expansion of *P. intestinalis* but not *P. rodentium* (Figure 5G). Increasing the dose of WAX to 20 g/l further enhanced the relative abundance of *P. intestinalis* 1 day after WAX addition to similar levels observed with Stand-PP (Figure 5H). In independent experiments after colonization of SPF-HZI mice with only

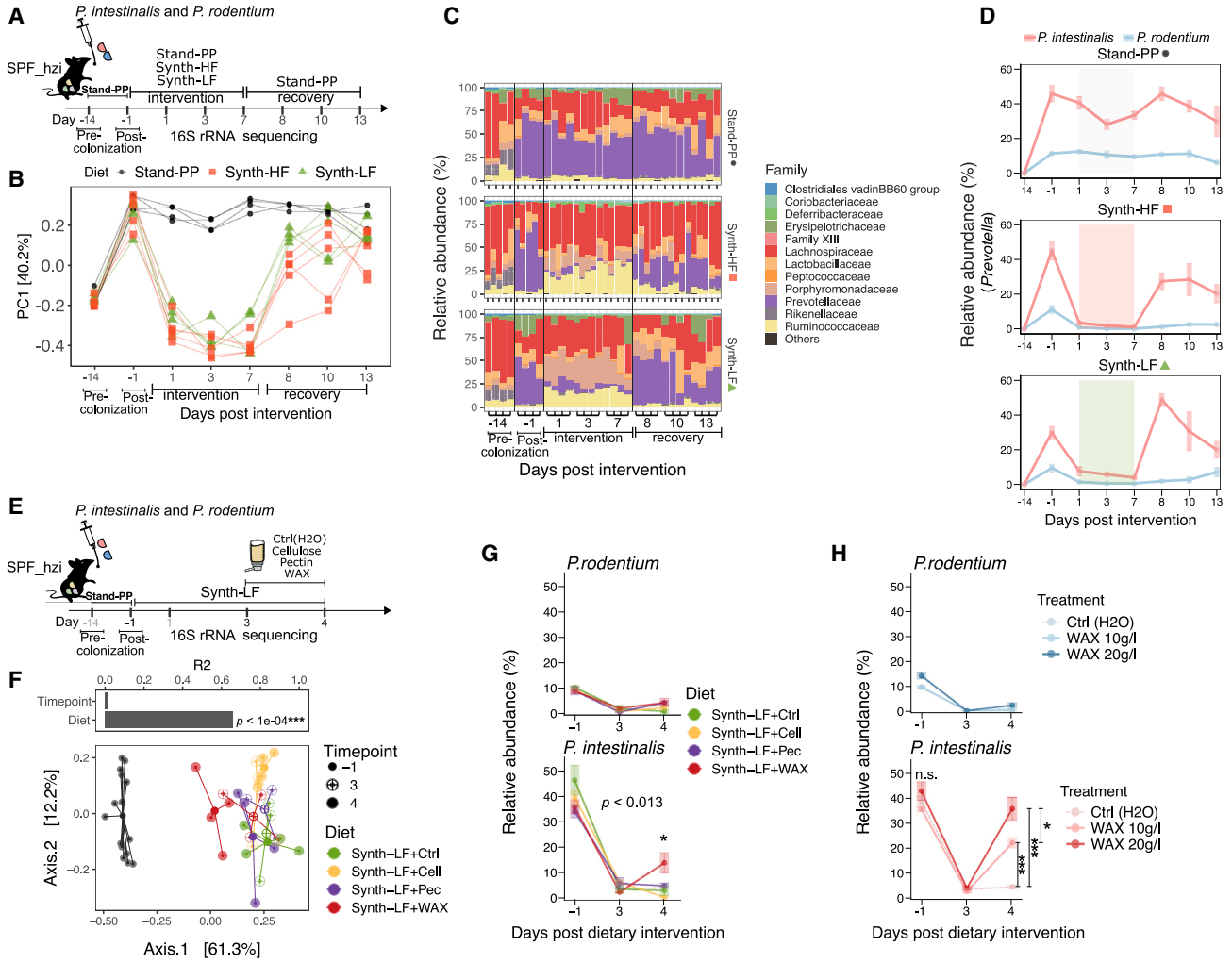

Figure 5. The Effect of Distinct Polysaccharides and Microbial Communities on the Dominance of *P. Intestinalis*

(A–D) Diet intervention in SPF_hzi mice colonized with *P. intestinalis* and *P. rodentium*.

(A) Experimental design for longitudinal diet interventions comparing standard chow (Stand-PP), a semi-synthetic diet rich in high fat (60%) (Synth-HF) and a control low in fat and rich in simple sugars (Synth-LF) (see STAR Methods; n = 4 animals/group).

(B) Changes in similarity of gut microbial communities using PCoA ordination analysis. Each shape represents a fecal sample from a mouse belonging to the indicated diet group; y axis indicates PCoA1 using Bray-Curtis distances, and x axis indicates the time point at which diet was switched.

(C) Relative abundance (%) of 15 most abundant bacterial families in individual samples. Samples are split by diet intervention and sorted by time point.

(D) Dynamics of relative abundance (%) of *P. intestinalis* (light red) and *P. rodentium* (light blue) upon diet intervention. Centers represent the mean value and error bars show ± SEM (n = 4 animals / group).

(E–H) Competition between *P. intestinalis* and *P. rodentium* upon complex polysaccharide supplementation.

(E) Experimental design for longitudinal competition experiment between P. intestinalis and P. rodentium.

(F) Variance effect size using ADONIS test and PCoA of gut microbiota composition using Bray-Curtis distances.

(G) Relative abundances (%) of *P. rodentium* and *P. intestinalis* in fecal samples from SPF_hzi mice fed with a controlled semisynthetic diet (Synth-LF) and supplemented with one of the 3 complex polysaccharides (Cell, Cellulose; Pec, Pectin; WAX, Wheat-arabinoxylan), n = 4 animals per treatment. *p < 0.05 (Kruskal-Wallis test).

(H) Relative abundances (%) of *P. intestinalis* versus *P. rodentium* during different dose of WAX supplementation. Ctrl (Synth-LF+H2O) compared with the WAX (10 g/l and 20 g/l supplemented in the drinking water). n = 7–10 animals per treatment. *p < 0.05 (Mann-Whitney U test).

See also Figure S4.

P. intestinalis, comparable results were obtained 3 days after WAX intervention. Notably, we followed here a slightly different sampling scheme, but the results still support that *P. intestinalis* does not benefit specifically of factors derived from *P. rodentium* (Figures S4E–S4G). To provide additional evidence that distinct polysaccharides can be directly utilized by *P. intestinalis*, we evaluated different media for their ability to support *P. intestinalis* DSM103738 growth only in presence of additional mono- or polysaccharides. While different minimal media utilized to study *Bacteroides spp.* (Martens et al., 2011; McNulty et al., 2013) and *P. copri* (Franke and Deppenmeier, 2018) were not able to support *P. intestinalis* growth after the

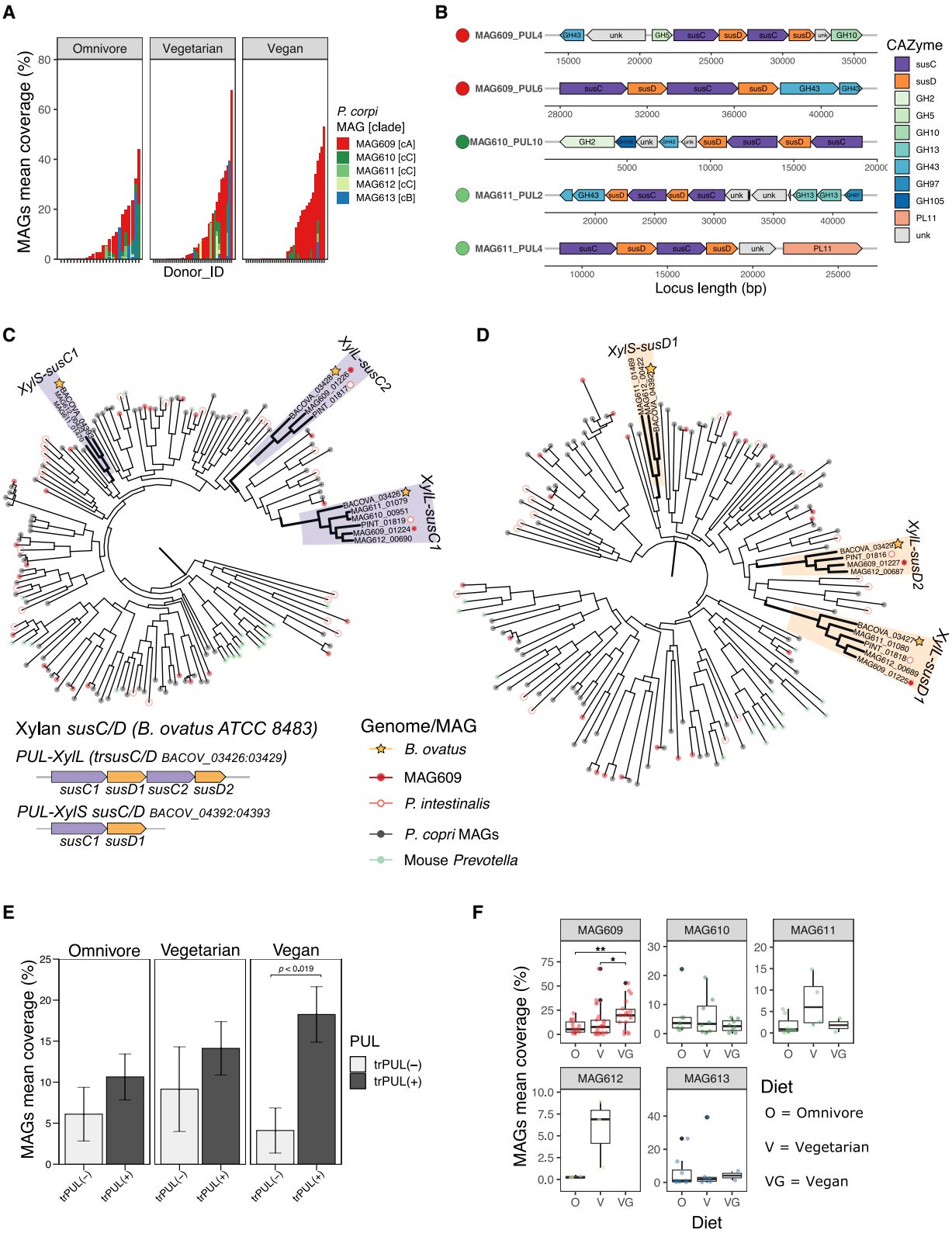

(legend on next page)

addition of glucose as an energy source, YCFA in combination with glucose, xylose, or arabinose supported the growth. We then evaluated the ability of WAX, cellulose, pectin, starch, or rhamnogalacturonan as carbon sources *in vitro*. In line with the *in vivo* observations, WAX was able to consistently boost the growth of *P. intestinalis in vitro*, while cellulose, starch, or rhamnogalacturonan did not support growth (Figures S4H and S4I). Notably, pectin supported growth *in vitro*, but not *in vivo*, at the time points tested. Together, these experiments demonstrate that utilization of dietary WAX, potentially via *trsusC/D* elements, allows the expansion of *P. intestinalis* even in Westernized diets.

Prevotella copri Strains with a Broad Repertoire of (Arabino)xylan PULs Dominate the Human Gut Microbiome

In the human gut microbiome, multiple *P. copri* clades as well as other *Prevotella* spp. can co-exist and compete (Tett et al., 2019). Yet, whether differential abilities to utilize xylans are potentially linked to the expansion of specific strains of *P. copri* is not known. Hence, we aimed to characterize whether specific *P. copri* strains dominate or are more abundant than other *P. copri* strains in the presence of specific diets. Therefore, a publicly available data set from a recent study investigating the microbiota in individuals consuming different diets (omnivore, vegetarian, and vegan) (n = 101 individuals) was reanalyzed (Figure S5A) (De Filippis et al., 2019). Sample wise-assembly was performed using the ATLAS workflow (Kieser et al., 2019; see STAR Methods for parameters). Assembly, binning, dereplication, and classification of MAGs resulted in 34 different high-quality MAGs (completeness >90%; contamination <10%) putatively belonging to the family Prevotellaceae (Table S6). Phylogenetic analysis using reference genomes of *P. copri* isolates from all four clades allowed us to identify that 5/34 dereplicated MAGs belonged to the *P. copri* complex (Figures S5B and S5C), with the rest belonging to other species from the Prevotellaceae family. The *P. copri* MAGs clustered within clade A (MAG609), clade B (MAG613), and clade C (MAG610, MAG611, and MAG612). Analysis of the relative abundance of these MAGs identified a single MAG, i.e., MAG609, as highly abundant and prevalent across the samples, especially in vegans and vegetarians (Figure 6A). Next, we wanted to identify if *P. copri* MAGs shared homolog putative (arabino)xylan (PULs with *P. intestinalis*. Hence, a genome-wide prediction of CAZymes and *susC/susD* genes for all identified *P. copri* MAGs was conducted followed by phylogenetic analysis with the previously characterized mouse *Prevotella susC/susD* genes (Figures 6B–6D). In parallel, we specifically searched for *trsusC/D* elements within the MAGs identifying 5 distinct *trsusC/D* elements, two each in MAG609 and MAG611, as well as one in MAG610 (Figure 6B; Table S6). The structure and composition of CAZymes (GH43, GH10, GH5, and PL1) indicate their potential affinity for arabinoxylans and pectins (Gilbert, 2010; Luis et al., 2018; Rogowski et al., 2015). Of note, for the global phylogenetic analysis, the well-characterized xylan/arabinoxylan systems of *Bacteroides ovatus* composed by a *trsusC/D* (PUL-XylL; BACOV_03426: BACOV_03429), which is activated by complex forms of the hemicellulose, and a single *susC/D* pair (PUL-XylS; BACOV_04392: BACOV_04393) activated with simple linear xylans, was included as a reference (Rogowski et al., 2015). Strikingly, only MAG609 and *P. intestinalis* shared homologs of both *susC/D* pairs of the PUL-XylL, while the other MAGs and murine *Prevotella* species did only partly or not at all, respectively, shared these elements (Figures 6C and 6D). To further understand the association between *trsusC/D* and dominance of *Prevotella* spp., the *P. copri* MAGs were classified into two distinct groups according to the presence or absence of *trsusC/D*, and the relative abundance of each group (percentage of MAG coverage mean) was calculated for each dietary preference. Strikingly, *trsusC/D*(+) MAGs were characterized by a higher relative abundance compared with MAGs without *trsusC/D*(−) in all three diets, yet, most pronounced in individuals consuming a vegan diet, the equivalent for the plant-based chow in mice (Figure 6E). Next, we analyzed the relative abundance of each of the MAGs according to the dietary preference and observed an expansion of *trsusC/D*(+) MAG609 in a vegan diet and, to a lower degree, also in a vegetarian diet (U-test; p value < 0.01 and p value < 0.05, respectively) (Figure 6F). Moreover, we observed the highest relative abundance of the *trsusC/D*(+) MAG611 in vegetarians, while the less prevalent *trsusC/D*(+) MAG610 and the *trsusC/D*(−) MAG612 and MAG613 did not display differences depending on the diets. In summary, a prevalent *P. copri* strain encoding a *trsusC/D*(+) PUL with high similarity to the xylan/arabinoxylan-degrading PUL in *B. ovatus* and being shared with *P. intestinalis*, but not other murine *Prevotella* spp., displays a diet-dependent increased abundance in the human gut.

DISCUSSION

Unexplored Diversity in the Genus *Prevotella* in the Mouse Gut Microbiome

The family Prevotellaceae (genus *Prevotella*) contains diverse bacteria that are part of complex host-associated microbial

Figure 6. Dominance of *P. copri* Metagenome-Assembled Genomes (MAGs) and Its Association with *Polysaccharide* Utilization Loci (PUL) in Distinct Diet Habits

(A) Relative abundance (%) of *P. copri* MAGs in each individual. Identification of *P. copri* MAGs and its clade-characterization performed by genome-based phylogenetic reconstruction (number of individuals n = 101; Figure S5).

(B) Schematic representation of predicted PULs with tandem-repeat *susC/D* genes (trsusC/*susD*) in *P. copri* MAGs.

(C and D) Phylogenetic tree of *susC* (C) and *susD* (D) amino-acid sequences from the isolated mouse *Prevotella* and the reconstructed *P. copri* MAGs. Each tree was constructed using RAxML algorithm with 1,000 bootstrap replicates. The well-characterized arabinoxylan utilization system of *B. ovatus* was used as reference. The system is composed of a large PUL (XylL) containing a *trsusC/D* and a short PUL (*XylS*) containing a single pair of *susC/D* elements. Colored branches (purple, *susC*; orange, susD) highlight the topology of the reference sequences from *B. ovatus* (stars) and colored shapes on the tips represent the genome/MAG source.

(E) Relative abundance (%) of *P. copri* MAGs encoding PULs with *trsusC/D*(+) versus *trsusC/D*(−). *p < 0.05 (t-test).

(F) Box-plot of MAGs relative abundance and its association with host dietary habit. *p < 0.05 (Mann-Whitney U test).

See also Figure S5; Table S6.

communities. Initial genomics studies of *Prevotella* isolates from various anatomical sites identified genetic divergence of *Prevotella* spp. according to their habitat, e.g., the gastrointestinal tract or the oropharynx (Gupta et al., 2015), yet, *Prevotella* spp. in small animal models important for biomedical research have not been explored in detail. Our genome- and metagenome-based phylogenetic analysis using isolates and data from a mouse metagenome catalog recently established by us (Lesker et al., 2020) identifies the presence of at least five distinct *Prevotella* species clusters with high relative abundances in laboratory and wild mice expanding the diversity in this genus. Of the five previously unknown species, we were able to successfully isolate and maintain several independent and genetically diverse isolates from three species, which are now available in a public depository. This expands the currently available strain collections, which so far lack the *Prevotella* isolates (Lagkouvardos et al., 2016; Liu et al., 2020) and will permit scientists to perform functional studies in mouse models. Enabled by the model systems and isolated strains, we performed controlled *Prevotella* spp. competition experiments *in vivo* to address the question whether the specific isolates from *Prevotella* spp. in mice compete or co-operate with each other in the gut. Our results demonstrated a strong inter-species antagonism between the tested isolates and that a specific isolate, i.e., *P. intestinalis* DSM103738, from the species complex *P. intestinalis*, outcompeted isolates from other *Prevotella* spp. as well as other commensals in different microbiome settings (Iljazovic et al., 2020). Of note, we performed these competition experiments using strains being representative for the species with respect to their CAZyme profiles, but future experiments will be required to investigate whether the observed phenotypes can be generalized for the other strains of these species as well. The domination of *P. intestinalis* DSM103738 is in contrast with what has been recently suggested for *P. copri* strains in humans based on *ex vivo* profiling of PULs and *susC/D* genes as well as the co-existence of multiple *P. copri* clades in some individuals (Fehlner-Peach et al., 2019). As *Prevotella* dominance is frequently observed in humans consuming plant-rich diets, multiple strains in the human gut may also compete for distinct polysaccharides or structural elements of polysaccharide, yet, this is difficult to resolve without appropriate experimental models. In the case of laboratory mice consuming a chow-based diet, which has likely a lower diversity of polysaccharide structures, we observed that each *Prevotella* species can individually efficiently expand in a *Prevotella*-free host, but one specific species outcompetes the others. Strikingly, the variable kinetic of the domination of *P. intestinalis* DSM103721 after the co-housing of mice, i.e., some microbiotas were rapidly colonized while others displayed delayed domination, suggests the existence of complex interactions with other commensals, which may also exist in humans. Again, the domination of a specific strain over strains from a different species cannot be generalized to the complete species complexes as strain diversity, and resulting functional variability is emerging to be a common theme not only in *Prevotella* spp. but also in other commensals (Fehlner-Peach et al., 2019; Sorbara et al., 2020; Tett et al., 2019). Additional cultivation and sequencing efforts will be needed to expand the collection of strains from the identified species, specifically from diverse hosts including wild mice. As investigations in humans are limited by the inability to experimentally expose individuals to multiple strains and species of *Prevotella* spp., our study provides an example on the utilization of these distinct *Prevotella* species and strains in experimental models for future validation of observations in human studies.

Prevotella Polysaccharide Utilization *In Vivo*

Genomic and functional studies have identified, predominantly, the degradation of plant-derived polysaccharides as an energy source for *Prevotella* spp. (Accetto and Avguštin, 2015; Dodd et al., 2011; Tan et al., 2018). In line with these observations, in our experiments replacing a diet rich in plant-derived polysaccharides with a semi-synthetic diet containing starch and indigestible cellulose as fiber resulted in stark reductions in the abundance of murine *Prevotella* spp. and the expansion of different families of bacteria, e.g., Muribaculaceae and Porphyromonadaceae. Littman and colleagues recently identified variations in the number and composition of PULs as one of the most evident genomic differences between *P. copri* strains (Fehlner-Peach et al., 2019). In our study, diversity between strains was typically lower than the diversity between different species. While all three *Prevotella* spp. were able to efficiently colonize the gut of mice on chow diet, the competition experiments revealed that a higher number of PULs were associated with the ability to outcompete other *Prevotella* spp. Of note, other genomic differences besides PULs may influence intestinal domination of *P. intestinalis* DSM103738 and will be of interest for future studies. Metatranscriptome analysis using RNA-seq resulted in the identification of multiple highly expressed PULs, including ones containing predicted pectin-degrading enzymes or another one contained xylanses and *trsusC/D* elements. Notably, gene expression of homologs of this PUL were induced *in vitro* in *P. bryantii* and *P. ruminicola* as well as *B. ovatus* during growth on soluble wheat arabinoxylan (Dodd et al., 2010, 2011; Martens et al., 2011; Rogowski et al., 2015). Hence, we hypothesized that either pectin- or xylan-related polysaccharides may be required for the expansion of *P. intestinalis* DSM103721 *in vivo*. Strikingly, WAX, but not pectin, was sufficient to support the expansion of *P. intestinalis* DSM103721 pointing to the critical role of xylan-related polysaccharides for *Prevotella* spp. The role of additional other structurally diverse polysaccharides (inulin, xylan, arabinan, pectic galactan, etc.) for *Prevotella* spp. competition and domination can now be explored using these and additional strains, which may lead to distinct strain-dependent effects. Interestingly, xylan-degrading enzymes are widely conserved in *P. copri* strains (Fehlner-Peach et al., 2019), but *trsusC/D* elements, which only represent a small fraction of PULs (Lapébie et al., 2019) in Bacteroidetes, were variably connected to xylan-degrading enzymes in *P. copri* strains (Fehlner-Peach et al., 2019). Our screening of *trsusC/D* in metagenomic human *P. copri* strains identified homologs of *trsusC/D* encoded by a prevalent *P. copri* MAG with a high relative abundance in individuals consuming a vegan diet. Other *P. copri* MAGs lacking *trsusC/D* elements did not display a comparable enrichment according to the diet. In *Bacteroides* spp., the expression of *trsusC/D* was associated with degradation of WAX and arabinan (Patnode et al., 2019), but these elements are not highly expressed *in vivo*, and recent studies have rather reported that

genetic variation of single *susC*/*susD* genes in *Bacteroides* spp. are determinates of interspecies competition and adaptive evolution (Joglekar et al., 2018; Zhao et al., 2019). The combination of the presence of *trsusC*/*D* and specific dietary polysaccharides is, thus, potentially an important factor contributing to the expansion of specific *P. copri* strains at the cost of other Bacteroidales including *Bacteroides* spp.

Implications

In the last decade, the presence and overexpansion of *Prevotella* spp. in the gut microbiome have been associated to both beneficial and detrimental outcomes on human health (Alpizar-Rodriguez et al., 2019; Kovatcheva-Datchary et al., 2015; Scher et al., 2013; De Vadder et al., 2016). Until recently, attempts to understand the puzzling biology of *Prevotella* species have been hindered mostly due to challenging cultivation, low number of publicly available isolates from human and model organisms, and lack of tools for genetic manipulation. Here, we provide a set of previously undescribed *Prevotella* species isolated from mice available for functional studies. We studied their metabolic niche and, through a combination of *in vivo* experiments in mice with the bioinformatic analysis of publicly available metagenomic sequencing data from human cohort studies, gained insights into the biology of *Prevotella* spp. This may serve as a framework for advancing the knowledge about these keystone species in the gut microbiota, yet, strain-specific phenotypes cannot be simply generalized to diverse species complexes. The eventual establishment of genetic tools for non-classical model organisms, such as *P. copri* and murine *Prevotella* spp., have the potential to further advance studies into their interspecies diversity, ecology, and metabolic role *in vivo*.

STAR★METHODS

Detailed methods are provided in the online version of this paper and include the following:

- KEY RESOURCES TABLE
- RESOURCE AVAILABILITY
  - Lead Contact
  - Materials Availability
  - Data and Code Availability
- EXPERIMENTAL MODEL AND SUBJECT DETAILS
  - Bacterial Strains
  - Mouse Strains
- METHOD DETAILS
  - *In Vitro* Polysaccharide Growth Assay
  - Total DNA Isolation and Whole Genome Sequencing
  - Genome Assembly and Annotation
  - 16S rRNA Amplification and Sequencing
  - 16S rRNA Analysis
  - Metagenomic Reconstruction of Mouse *Prevotella* MAGs
  - Phylogenetic Analyses
  - Automated Reconstruction of *P. copri* MAGs
  - PUL Analysis in *Prevotella* Genomes and MAGs
  - Total RNA Isolation and RNA-seq Library Preparation
  - Differential Gene Expression RNA-seq Analysis
  - Microbiota Manipulation and Diet Interventions
- QUANTIFICATION AND STATISTICAL ANALYSIS
  - Statistical Analysis

SUPPLEMENTAL INFORMATION

Supplemental Information can be found online at https://doi.org/10.1016/j.chom.2020.09.012.

ACKNOWLEDGMENTS

We thank the members of the Strowig laboratory for valuable discussions. We thank the staff of the animal unit and the genome analytics core facility at the Helmholtz Institute for Infection Research for excellent technical support. The project was kindly supported by the Helmholtz Association (#VH-NG-933 to T.S.) and by the Deutsche Forschungsgemeinschaft (DFG, German Research Foundation, projects STR-1343/1 and under Germany's Excellence Strategy – EXC 2155 "RESIST" – project ID 39087428).

AUTHOR CONTRIBUTIONS

E.J.C.G., A.I., and T.S. designed the experiments and wrote the manuscript with input from co-authors. E.J.C.G., A.I., L.A., S.T., L.H., U.R., and A.G. performed microbiological, genomics, and animal experiments. E.J.C.G., T.R.L., and T.R. performed the bioinformatics analysis. E.C. provided critical input, and T.S. supervised the study.

DECLARATION OF INTERESTS

The authors declare no competing interests.

Received: May 10, 2020
Revised: August 7, 2020
Accepted: September 16, 2020
Published: October 27, 2020

REFERENCES

Accetto, T., and Avguštin, G. (2015). Polysaccharide utilization locus and CAZYme genome repertoires reveal diverse ecological adaptation of Prevotella species. Syst. Appl. Microbiol. *38*, 453–461.

Alpizar-Rodriguez, D., Lesker, T.R., Gronow, A., Gilbert, B., Raemy, E., Lamacchia, C., Gabay, C., Finckh, A., and Strowig, T. (2019). Prevotella copri in individuals at risk for rheumatoid arthritis. Ann. Rheum. Dis. *78*, 590–593.

Amann, R.I., Binder, B.J., Olson, R.J., Chisholm, S.W., Devereux, R., and Stahl, D.A. (1990). Combination of 16S rRNA-targeted oligonucleotide probes with flow cytometry for analyzing mixed microbial populations. Appl. Environ. Microbiol. *56*, 1919–1925.

Anders, S., Pyl, P.T., and Huber, W. (2015). HTseq-a python framework to work with high-throughput sequencing data. Bioinformatics *31*, 166–169.

Asnicar, F., Thomas, A.M., Beghini, F., Mengoni, C., Manara, S., Manghi, P., Zhu, Q., Bolzan, M., Cumbo, F., May, U., et al. (2020). Precise phylogenetic analysis of microbial isolates and genomes from metagenomes using PhyloPhlAn 3.0. Nature Communications *11*, 2500.

Bankevich, A., Nurk, S., Antipov, D., Gurevich, A.A., Dvorkin, M., Kulikov, A.S., Lesin, V.M., Nikolenko, S.I., Pham, S., Prjibelski, A.D., et al. (2012). SPAdes: a new genome assembly algorithm and its applications to single-cell sequencing. J. Comput. Biol. *19*, 455–477.

Bjursell, M.K., Martens, E.C., and Gordon, J.I. (2006). Functional genomic and metabolic studies of the adaptations of a prominent adult human gut symbiont, Bacteroides thetaiotaomicron, to the suckling period. J. Biol. Chem. *281*, 36269–36279.

Boetzer, M., Henkel, C.V., Jansen, H.J., Butler, D., and Pirovano, W. (2011). Scaffolding pre-assembled contigs using SSPACE. Bioinformatics *27*, 578–579.

Bolger, A.M., Lohse, M., and Usadel, B. (2014). Trimmomatic: a flexible trimmer for Illumina sequence data. Bioinformatics *30*, 2114–2120.

Buchfink, B., Xie, C., and Huson, D.H. (2015). Fast and sensitive protein alignment using DIAMOND. Nat. Methods *12*, 59–60.

Capella-Gutiérrez, S., Silla-Martínez, J.M., and Gabaldón, T. (2009). trimAl: a tool for automated alignment trimming in large-scale phylogenetic analyses. Bioinformatics *25*, 1972–1973.

Caporaso, J.G., Lauber, C.L., Walters, W.A., Berg-Lyons, D., Lozupone, C.A., Turnbaugh, P.J., Fierer, N., and Knight, R. (2011). Global patterns of 16S rRNA diversity at a depth of millions of sequences per sample. Proc. Natl. Acad. Sci. USA *108*, 4516–4522.

Chaumeil, P.A., Mussig, A.J., Hugenholtz, P., and Parks, D.H. (2019). GTDB-Tk: a toolkit to classify genomes with the genome taxonomy database. Bioinformatics.

Chen, T., Long, W., Zhang, C., Liu, S., Zhao, L., and Hamaker, B.R. (2017). Fiber-utilizing capacity varies in Prevotella- versus Bacteroides-dominated gut microbiota. Sci. Rep. *7*, 2594.

Clemente, J.C., Pehrsson, E.C., Blaser, M.J., Sandhu, K., Gao, Z., Wang, B., Magris, M., Hidalgo, G., Contreras, M., Noya-Alarcón, Ó., et al. (2015). The microbiome of uncontacted Amerindians. Sci. Adv. *1*, e1500183.

Costea, P.I., Hildebrand, F., Manimozhiyan, A., Bäckhed, F., Blaser, M.J., Bushman, F.D., De Vos, W.M., Ehrlich, S.D., Fraser, C.M., Hattori, M., et al. (2017). Enterotypes in the landscape of gut microbial community composition. Nat. Microbiol. *3*, 8–16.

David, L.A., Maurice, C.F., Carmody, R.N., Gootenberg, D.B., Button, J.E., Wolfe, B.E., Ling, A.V., Devlin, A.S., Varma, Y., Fischbach, M.A., et al. (2014). Diet rapidly and reproducibly alters the human gut microbiome. Nature *505*, 559–563.

De Filippis, F., Pasolli, E., Tett, A., Tarallo, S., Naccarati, A., De Angelis, M., Neviani, E., Cocolin, L., Gobbetti, M., Segata, N., et al. (2019). Distinct genetic and functional traits of human intestinal Prevotella copri Strains Are associated with different habitual diets. Cell Host Microbe *25*, 444–453.e3.

De Vadder, F., Kovatcheva-Datchary, P., Zitoun, C., Duchampt, A., Bäckhed, F., and Mithieux, G. (2016). Microbiota-produced succinate improves glucose homeostasis via intestinal gluconeogenesis. Cell Metab. *24*, 151–157.

Dillon, S.M., Lee, E.J., Kotter, C.V., Austin, G.L., Dong, Z., Hecht, D.K., Gianella, S., Siewe, B., Smith, D.M., Landay, A.L., et al. (2014). An altered intestinal mucosal microbiome in HIV-1 infection is associated with mucosal and systemic immune activation and endotoxemia. Mucosal Immunol. *7*, 983–994.

Dobin, A., Davis, C.A., Schlesinger, F., Drenkow, J., Zaleski, C., Jha, S., Batut, P., Chaisson, M., and Gingeras, T.R. (2013). STAR: ultrafast universal RNA-seq aligner. Bioinformatics *29*, 15–21.

Dodd, D., Mackie, R.I., and Cann, I.K.O. (2011). Xylan degradation, a metabolic property shared by rumen and human colonic Bacteroidetes. Mol. Microbiol. *79*, 292–304.

Dodd, D., Moon, Y.H., Swaminathan, K., Mackie, R.I., and Cann, I.K.O. (2010). Transcriptomic analyses of xylan degradation by Prevotella bryantii and insights into energy acquisition by xylanolytic Bacteroidetes. J. Biol. Chem. *285*, 30261–30273.

Eddy, S.R. (2011). Accelerated Profile HMM Searches. PLoS Comput Biol *7*, e1002195.

Edgar, R.C. (2013). Uparse: highly accurate OTU sequences from microbial amplicon reads. Nat. Methods *10*, 996–998.

Elinav, E., Strowig, T., Kau, A.L., Henao-Mejia, J., Thaiss, C.A., Booth, C.J., Peaper, D.R., Bertin, J., Eisenbarth, S.C., Gordon, J.I., and Flavell, R.A. (2011). NLRP6 inflammasome regulates colonic microbial ecology and risk for colitis. Cell *145*, 745–757.

Fehlner-Peach, H., Magnabosco, C., Raghavan, V., Scher, J.U., Tett, A., Cox, L.M., Gottsegen, C., Watters, A., Wiltshire-Gordon, J.D., Segata, N., et al. (2019). Distinct polysaccharide utilization profiles of human intestinal Prevotella copri isolates. Cell Host Microbe *26*, 680–690.e5.

Franke, T., and Deppenmeier, U. (2018). Physiology and central carbon metabolism of the gut bacterium Prevotella copri. Mol. Microbiol. *109*, 528–540.

Gálvez, E.J.C., Iljazovic, A., Gronow, A., Flavell, R., and Strowig, T. (2017). Shaping of intestinal microbiota in Nlrp6- and Rag2-deficient mice depends on community structure. Cell Rep. *21*, 3914–3926.

Gilbert, H.J. (2010). Update on structure of cell wall-degrading enzymes: the biochemistry and structural biology of plant cell wall deconstruction. Plant Physiol. *153*, 444–455.

Gorvitovskaia, A., Holmes, S.P., and Huse, S.M. (2016). Interpreting Prevotella and Bacteroides as biomarkers of diet and lifestyle. Microbiome *4*, 15.

Gupta, V.K., Chaudhari, N.M., Iskepalli, S., and Dutta, C. (2015). Divergences in gene repertoire among the reference Prevotella genomes derived from distinct body sites of human. BMC Genomics *16*, 153.

Hayashi, H., Shibata, K., Sakamoto, M., Tomita, S., and Benno, Y. (2007). Prevotella copri sp. nov. and Prevotella stercorea sp. nov., isolated from human faeces. Int. J. Syst. Evol. Microbiol. *57*, 941–946.

Human Microbiome Project Consortium (2012). Structure, function and diversity of the healthy human microbiome. Nature *486*, 207–214.

Iljazovic, A., Roy, U., Gálvez, E.J.C., Lesker, T.R., Zhao, B., Gronow, A., Amend, L., Will, S.E., Hofmann, J.D., Pils, M.C., et al. (2020). Perturbation of the gut microbiome by Prevotella spp. enhances host susceptibility to mucosal inflammation. Mucosal Immunol. https://doi.org/10.1038/s41385-020-0296-4.

Joglekar, P., Sonnenburg, E.D., Higginbottom, S.K., Earle, K.A., Morland, C., Shapiro-Ward, S., Bolam, D.N., and Sonnenburg, J.L. (2018). Genetic variation of the SusC/SusD homologs from a polysaccharide utilization locus underlies divergent fructan specificities and functional adaptation in bacteroides thetaiotaomicron strains. mSphere *3*, e00185-18.

Katoh, K., and Standley, D.M. (2013). MAFFT multiple sequence alignment software version 7: improvements in performance and usability. Mol. Biol. Evol. *30*, 772–780.

Kieser, S., Brown, J., Zdobnov, E.M., Trajkovski, M., and McCue, L.A. (2019). Atlas: a Snakemake workflow for assembly, annotation, and genomic binning of metagenome sequence data. NOW BMC Bioinformatics. https://doi.org/10.1186/s12859-020-03585-4.

Koropatkin, N.M., Cameron, E.A., and Martens, E.C. (2012). How glycan metabolism shapes the human gut microbiota. Nat. Rev. Microbiol. *10*, 323–335.

Kovatcheva-Datchary, P., Nilsson, A., Akrami, R., Lee, Y.S., De Vadder, F., Arora, T., Hallen, A., Martens, E., Björck, I., and Bäckhed, F. (2015). Dietary fiber-induced improvement in glucose metabolism is associated with increased abundance of Prevotella. Cell Metab. *22*, 971–982.

Lagkouvardos, I., Pukall, R., Abt, B., Foesel, B.U., Meier-Kolthoff, J.P., Kumar, N., Bresciani, A., Martínez, I., Just, S., Ziegler, C., et al. (2016). The mouse intestinal bacterial collection (miBC) provides host-specific insight into cultured diversity and functional potential of the gut microbiota. Nat. Microbiol. *1*, 16131.

Lapébie, P., Lombard, V., Drula, E., Terrapon, N., and Henrissat, B. (2019). Bacteroidetes use thousands of enzyme combinations to break down glycans. Nat. Commun. *10*, 2043.

Lesker, T.R., Durairaj, A.C., Gálvez, E.J.C., Lagkouvardos, I., Baines, J.F., Clavel, T., Sczyrba, A., McHardy, A.C., and Strowig, T. (2020). An integrated metagenome catalog reveals new insights into the murine gut microbiome. Cell Rep. *30*, 2909–2922.e6.

Li, M., Zhou, H., Hua, W., Wang, B., Wang, S., Zhao, G., Li, L., Zhao, L., and Pang, X. (2009). Molecular diversity of Bacteroides spp. in human fecal microbiota as determined by group-specific 16S rRNA gene clone library analysis. Syst. Appl. Microbiol. *32*, 193–200.

Liu, C., Zhou, N., Du, M.X., Sun, Y.T., Wang, K., Wang, Y.J., Li, D.H., Yu, H.Y., Song, Y., Bai, B.-B., et al. (2020). The mouse gut microbial biobank expands the coverage of cultured bacteria. Nat. Commun. *11*, 79.

Lombard, V., Golaconda Ramulu, H., Drula, E., Coutinho, P.M., and Henrissat, B. (2014). The carbohydrate-active enzymes database (CAZy) in 2013. Nucleic Acids Res. *42*, D490–D495.

Love, M.I., Huber, W., and Anders, S. (2014). Moderated estimation of fold change and dispersion for RNA-seq data with DESeq2. Genome Biol. *15*, 550.

Luis, A.S., Briggs, J., Zhang, X., Farnell, B., Ndeh, D., Labourel, A., Baslé, A., Cartmell, A., Terrapon, N., Stott, K., et al. (2018). Dietary pectic glycans are degraded by coordinated enzyme pathways in human colonic Bacteroides. Nat. Microbiol. *3*, 210–219.

Martens, E.C., Lowe, E.C., Chiang, H., Pudlo, N.A., Wu, M., McNulty, N.P., Abbott, D.W., Henrissat, B., Gilbert, H.J., Bolam, D.N., and Gordon, J.I. (2011). Recognition and degradation of plant cell wall polysaccharides by two human gut symbionts. PLoS Biol. *9*, e1001221.

Martínez, I., Stegen, J.C., Maldonado-Gómez, M.X., Eren, A.M., Siba, P.M., Greenhill, A.R., and Walter, J. (2015). The gut microbiota of rural Papua New Guineans: composition, diversity patterns, and ecological processes. Cell Rep. *11*, 527–538.

Matsuki, T., Watanabe, K., Fujimoto, J., Takada, T., and Tanaka, R. (2004). Use of 16S rRNA gene-targeted group-specific primers for real-time PCR analysis of predominant bacteria in human feces. Appl. Environ. Microbiol . *70*, 7220–7228.

McMurdie, P.J., and Holmes, S. (2013). phyloseq: an R package for Reproducible Interactive Analysis and Graphics of microbiome Census Data. PLoS One *8*, e61217.

McNulty, N.P., Wu, M., Erickson, A.R., Pan, C., Erickson, B.K., Martens, E.C., Pudlo, N.A., Muegge, B.D., Henrissat, B., Hettich, R.L., and Gordon, J.I. (2013). Effects of diet on resource utilization by a model human gut microbiota containing Bacteroides cellulosilyticus WH2, a symbiont with an extensive glycobiome. PLoS Biol. *11*, e1001637.

Miller, C.S., Handley, K.M., Wrighton, K.C., Frischkorn, K.R., Thomas, B.C., and Banfield, J.F. (2013). Short-read assembly of full-length 16S amplicons reveals bacterial diversity in subsurface sediments. PLoS One *8*, e56018, https://doi.org/10.1371/journal.pone.005601.

Ndeh, D., Rogowski, A., Cartmell, A., Luis, A.S., Baslé, A., Gray, J., Venditto, I., Briggs, J., Zhang, X., Labourel, A., et al. (2017). Complex pectin metabolism by gut bacteria reveals novel catalytic functions. Nature *544*, 65–70.

Nguyen, L.T., Schmidt, H.A., von Haeseler, A., and Minh, B.Q. (2015). IQ-TREE: a fast and effective stochastic algorithm for estimating maximum-likelihood phylogenies. Mol. Biol. Evol. *32*, 268–274.

Nurk, S., Bankevich, A., Antipov, D., Gurevich, A.A., Korobeynikov, A., Lapidus, A., Prjibelski, A.D., Pyshkin, A., Sirotkin, A., Sirotkin, Y., et al. (2013). Assembling single-cell genomes and mini-metagenomes from chimeric MDA products. J. Comput. Biol. *20*, 714–737.

Olm, M.R., Brown, C.T., Brooks, B., and Banfield, J.F. (2017). dRep: a tool for fast and accurate genomic comparisons that enables improved genome recovery from metagenomes through de-replication. ISME J. *11*, 2864–2868.

Patnode, M.L., Beller, Z.W., Han, N.D., Cheng, J., Peters, S.L., Terrapon, N., Henrissat, B., Le Gall, S., Saulnier, L., Hayashi, D.K., et al. (2019). Interspecies competition impacts targeted manipulation of human gut bacteria by fiber-derived glycans. Cell *179*, 59–73.e13.

Price, M.N., Dehal, P.S., and Arkin, A.P. (2010). FastTree 2 - approximately maximum-likelihood trees for large alignments. PLoS One *5*, e9490.

Quast, C., Pruesse, E., Yilmaz, P., Gerken, J., Schweer, T., Yarza, P., Peplies, J., and Glöckner, F.O. (2013). The SILVA ribosomal RNA gene database project: improved data processing and web-based tools. Nucleic Acids Res. *41*, D590–D596.

R Core Team (2019). R: a language and environment for statistical computing. https://www.R-project.org/.

Rakoff-Nahoum, S., Foster, K.R., and Comstock, L.E. (2016). The evolution of cooperation within the gut microbiota. Nature *533*, 255–259.

Ridaura, V.K., Faith, J.J., Rey, F.E., Cheng, J., Duncan, A.E., Kau, A.L., Griffin, N.W., Lombard, V., Henrissat, B., Bain, J.R., et al. (2013). Gut microbiota from twins discordant for obesity modulate metabolism in mice. Science *341*, 1241214.

Rogowski, A., Briggs, J.A., Mortimer, J.C., Tryfona, T., Terrapon, N., Lowe, E.C., Baslé, A., Morland, C., Day, A.M., Zheng, H., et al. (2015). Glycan complexity dictates microbial resource allocation in the large intestine. Nat. Commun. *6*, 7481.

Scher, J.U., Sczesnak, A., Longman, R.S., Segata, N., Ubeda, C., Bielski, C., Rostron, T., Cerundolo, V., Pamer, E.G., Abramson, S.B., et al. (2013). Expansion of intestinal Prevotella copri correlates with enhanced susceptibility to arthritis. eLife *2*, e01202.

Seemann, T. (2014). Prokka: rapid prokaryotic genome annotation. Bioinformatics *30*, 2068–2069.

Sorbara, M.T., Littmann, E.R., Fontana, E., Moody, T.U., Kohout, C.E., Gjonbalaj, M., Eaton, V., Seok, R., Leiner, I.M., and Pamer, E.G. (2020). Functional and genomic variation between human-derived isolates of Lachnospiraceae reveals inter- and intra-species diversity. Cell Host Microbe *28*, 134–146.e4.

Stamatakis, A. (2014). RAxML version 8: a tool for phylogenetic analysis and post-analysis of large phylogenies. Bioinformatics *30*, 1312–1313.

Stewart, R.D., Auffret, M.D., Roehe, R., and Watson, M. (2018). Open prediction of polysaccharide utilisation loci (PUL) in 5414 public Bacteroidetes genomes using PULpy. bioRxiv https://www.biorxiv.org/content/10.1101/421024v1.full.

Tan, H., Zhao, J., Zhang, H., Zhai, Q., and Chen, W. (2018). Isolation of low-abundant Bacteroidales in the human intestine and the analysis of their differential utilization based on plant-derived polysaccharides. Front. Microbiol. *9*, 1319.

Tett, A., Huang, K.D., Asnicar, F., Fehlner-Peach, H., Pasolli, E., Karcher, N., Armanini, F., Manghi, P., Bonham, K., Zolfo, M., et al. (2019). The prevotella copri complex comprises four distinct clades underrepresented in westernized populations. Cell Host Microbe *26*, 666–679.e7.

Thiemann, S., Smit, N., Roy, U., Lesker, T.R., Gálvez, E.J.C., Helmecke, J., Basic, M., Bleich, A., Goodman, A.L., Kalinke, U., et al. (2017). Enhancement of IFNγ production by distinct commensals ameliorates Salmonella-induced disease. Cell Host Microbe *21*, 682–694.e5.

von Meijenfeldt, F.A.B., Arkhipova, K., Cambuy, D.D., Coutinho, F.H., and Dutilh, B.E. (2019). Robust taxonomic classification of uncharted microbial sequences and bins with CAT and BAT. Genome Biol. *20*, 217.

Wang, Q., Garrity, G.M., Tiedje, J.M., and Cole, J.R. (2007). Naive bayesian classifier for rapid assignment of rRNA sequences into the new bacterial taxonomy. Appl. Environ. Microbiol. *73*, 5261–5267.

Wells, P.M., Adebayo, A.S., Freidin, M.B., Finckh, A., Strowig, T., Lesker, T.R., Alpizar-Rodriguez, D., Gilbert, B., Kirkham, B., Cope, A.P., et al. (2019). A polygenic risk score for rheumatoid arthritis sheds light on the Prevotella association. MedRxiv. https://doi.org/10.1016/S2665-9913(20)30064-3 https://www.medrxiv.org/content/10.1101/2019.12.09.19014183v1.

Wen, C., Zheng, Z., Shao, T., Liu, L., Xie, Z., Le Chatelier, E., He, Z., Zhong, W., Fan, Y., Zhang, L., et al. (2017). Quantitative metagenomics reveals unique gut microbiome biomarkers in ankylosing spondylitis. Genome Biol. *18*.

Wickham, H. (2016). ggplot2: elegant graphics for data analysis (Springer-Verlag).

Wu, G.D., Chen, J., Hoffmann, C., Bittinger, K., Chen, Y.Y., Keilbaugh, S.A., Bewtra, M., Knights, D., Walters, W.A., Knight, R., et al. (2011). Linking long-term dietary patterns with gut microbial enterotypes. Science *334*, 105–108.

Yu, G., Lam, T.T.-Y., Zhu, H., and Guan, Y. (2018). Two methods for mapping and visualizing associated data on phylogeny using Ggtree. Mol. Biol. Evol. *35*, 3041–3043.

Zhang, H., Yohe, T., Huang, L., Entwistle, S., Wu, P., Yang, Z., Busk, P.K., Xu, Y., and Yin, Y. (2018). dbCAN2: a meta server for automated carbohydrate-active enzyme annotation. Nucleic Acids Res. *46*, W95–W101.

Zhao, S., Lieberman, T.D., Poyet, M., Kauffman, K.M., Gibbons, S.M., Groussin, M., Xavier, R.J., and Alm, E.J. (2019). Adaptive evolution within gut microbiomes of healthy people. Cell Host Microbe *25*, 656–667.e8.

STAR★METHODS

KEY RESOURCES TABLE

REAGENT or RESOURCE	SOURCE	IDENTIFIER
Bacterial and Virus Strains		
Prevotella sp. nov. strain PINT (referred to as Prevotella intestinalis)	This study	DSMZ, Cat#DSM103738
Prevotella sp. nov. strain PROD (referred to as Prevotella rodentium)	This study	DSMZ, Cat#DSM103721
Prevotella sp. nov. strain PMUR (referred to as Prevotella muris)	This study	DSMZ, Cat#DSM103722
Chemicals, Peptides, and Recombinant Proteins		
Carboxymethyl Cellulose	Megazyme	Cat#P-CMC4M
Pectin from Apples	Fluka	Cat#76282
Rhamnogalacturonan from soy bean	Megazyme	Cat#P-RHAGN
starch from potato	Sigma-Aldrich	Cat#33615-250G
Wheat Arabinoxylan RS	Megazyme	Cat#P-WAXYRS
D-(+)-Glucose	Sigma-Aldrich	Cat#G8270-1KG
D-(-)-Fructose	Sigma-Aldrich	Cat#F0127-100G
L-(+)-Arabinose	Sigma-Aldrich	Cat#A3256-25G
D-(+)-Xylose	Sigma-Aldrich	Cat#W360600
Brain Heart Infusion	Oxoid	Cat#CM1135
Bacto Agar	BD Bioscience	Cat#214010
Fetal Bovine Serum	Sigma-Aldrich	Cat#F7524
Menadione crystalline	Sigma-Aldrich	Cat#M5625-25G
Sheep blood defibrinated	Thermo Fisher Scientific	Cat#SR0051E
Bacto Casitone	BD Bioscience	Cat#225930
Yeast extract	Carl Roth	Cat#2363,3
NaCl	Carl Roth	Cat#3957,2
MgSO4 x 7H20	Carl Roth	Cat#P027.2
Cacl2	Sigma-Aldrich	Cat#223506-500G
Hemin	Sigma	Cat#H9039-1G
KH2PO4	Carl Roth	Cat#3904,1
K2HPO4	Merck	Cat#7758-11-4
NaHCO3	Merck	Cat#6329
(NH4)2SO4	Sigma	Cat#A4418-100G
Biotin	Sigma-Aldrich	Cat#B4501-100MG
Vitamin B12	Sigma	Cat#V2876-250MG
4-Aminobenzoic acid	Sigma	Cat#A9878-5G
Folic acid	Sigma	Cat#F7876-1G
Pyrodoxine hydrochloride	Sigma-Aldrich	Cat#47862
thiamine	Sigma	Cat#T-4625
Riboflavin	Sigma	Cat#R-4500
Acetic acid	Carl Roth	Cat#3738,5
Propionic acid	Sigma-Aldrich	Cat#402907-100ML
Isobutyric acid	Sigma	Cat#I1754-100ML
Isovaleric acid	Sigma-Aldrich	Cat#129542-100ML
n-valeric acid	Sigma-Aldrich	Cat#240370-100ML

(*Continued on next page*)

Continued

REAGENT or RESOURCE	SOURCE	IDENTIFIER
Critical Commercial Assays		
NEBNext® Ultra™ DNA Library Prep Kit for Illumina®	New England Biolabs	Cat#E7370S
NEBNext® Ultra™ Directional RNA Library Prep Kit for Illumina	New England Biolabs	Cat#E7420S
NEBNext® Multiplex Oligos for Illumina® (Index Primers Set 1)	New England Biolabs	Cat#E7335S
Ribo-Zero Gold rRNA Removal Kit (Epidemiology) (24 reactions)	Illumina	Cat#MRZE724
Agencourt® AMPure® XP Beads	Beckman Coulter, Inc.	Cat#A63880
Deposited Data		
Mouse Prevotella isolate genomes	This study	NCBI-BioProject: NCBI:PRJNA630669
Raw sequencing data	This study	NCBI-BioProject: NCBI:PRJNA630669
Code repository	This study	https://github.com/strowig-lab/galvez_et_al_2020/
Human gut metagenome from distinct diets	De Filippis et al., 2019	NCBI SRA: SRP126540 and SRP083099.
Experimental Models: Organisms/Strains		
Mouse, C57Bl6/N	Multiple providers (see Table S1)	N/A
Mouse, C57Bl6/N Nlrp6-/-	(Elinav et al., 2011; Gálvez et al., 2017)	N/A
Oligonucleotides		
Prevo-PINT-181f 5'-CGTCCCTTGACGGCATCCGACA-3'	This study	N/A
Prevo-PINT-1032r 5'-CAGCCCCGAAGGGAAGGGGTG-3'	This study	N/A
Prevo-PROD-603f 5'-TGAAATGTCGGGGCTCAACCTTGACAC-3'	This study	N/A
Prevo-PROD-1289r 5'-GCGGCTTTACGGATTGGACGTACG-3'	This study	N/A
Prevo-PMUR-61 5'-GGCAGCATGACATGTTTTCGGACGT-3'	This study	N/A
Prevo-PMUR-642r 5'-CAGTTCGCGCTGCAGGACCG-3'	This study	N/A
g-Prevo-F 5'-CACRGTAAACGATGGATGCC-3'	Matsuki et al., 2004	N/A
g-Prevo-R 5'-GGTCGGGTTGCAGACC-3'	Matsuki et al., 2004	N/A
Uni_334F 5'-ACTCCTACGGGAGGCAGCAGT-3'	Amann et al., 1990	N/A
Uni_514R 5'-ATTACCGCGGCTGCTGGC-3'	Amann et al., 1990	N/A
27F 5'-AGAGTTTGATCCTGGCTCAG-3'	Miller et al., 2013	N/A
1492R 5'-GGTTACCTTGTTACGACTT-3'	Miller et al., 2013	N/A
Software and Algorithms		
SPAdes (version 3.10.0)	Nurk et al., 2013	https://github.com/ablab/spades/releases
Prokka (version 1.13)	Seemann, 2014	https://github.com/tseemann/prokka
PhyloPhlAn (version dev commit b626e2dae732)	Asnicar et al., 2020	https://bitbucket.org/nsegata/phylophlan
MAFFT (version 7.310)	Katoh and Standley, 2013	https://github.com/The-Bioinformatics-Group/
FastTree (version 2.1.10)	Price et al., 2010	https://github.com/PavelTorgashov/FastTree
RAxML (version 8.1.15)	Stamatakis, 2014	https://github.com/stamatak/standard-RAxML

(*Continued on next page*)

CellPress

Continued

REAGENT or RESOURCE	SOURCE	IDENTIFIER
HMMSEARCH (version 3.1b2)	Eddy, 2011	https://github.com/guyz/HMM
Trimmomatic (version 0.33)	Bolger et al., 2014	http://www.usadellab.org/cms/?page=trimmomatic
STAR (version 2.5.2a)	Dobin et al., 2013	https://github.com/alexdobin/STAR
HTseq (version 0.11.2.)	Anders et al., 2015	https://github.com/htseq/htseq
DEseq2 (version 1.26.0.)	Love et al., 2014	https://bioconductor.org/packages/release/bioc/html/DESeq2.html
PULpy (commit 8955cdb)	Stewart et al., 2018	https://github.com/WatsonLab/PULpy
dbCAN2 (version 2.0.6)	Zhang et al., 2018	https://github.com/linnabrown/run_dbcan
ATLAS metagenomic workflow (version 2.1.3, commit a007857)	Kieser et al., 2019	https://github.com/metagenome-atlas/atlas
Usearch8 (version 8.1)	Edgar, 2013	https://www.drive5.com/usearch/
Other		
(Stand-PP) Rat/Mouse maintenance diet	Ssniff	Cat#V1534-300
(Synth-HF) Semi-synthetic rodent diet with 45 kcal % fat	Ssniff	Cat#D12451
(Synth-LF) LF Control diet for rodents with 10 kcal % Fat	Ssniff	Cat#D12450B

RESOURCE AVAILABILITY

Lead Contact

Further information and requests for resources and reagents should be directed to and will be fulfilled by the Lead Contact, Till Strowig (till.strowig@helmholtz-hzi.de). All unique reagents generated in this study are available from the Lead Contact without restriction.

Materials Availability

The *Prevotella* strains are available without restrictions from the German Collection of Microorganisms and Cell Cultures GmbH.

Data and Code Availability

The code developed to analyse the data has been deposited at https://github.com/strowig-lab/galvez_et_al_2020/. The data are available under NCBI-BioProject: NCBI:PRJNA630669.

EXPERIMENTAL MODEL AND SUBJECT DETAILS

Bacterial Strains

Bacterial strains used in the study are listed in the Key Resources Table. Isolation of *Prevotella* species was performed as previously described (Iljazovic et al., 2020). In brief, intestinal content from individual mice (6-10 weeks old) from distinct mouse lines (*Nlrp6*$^{-/-}$, SPF_jan and SPF_nci mice) that were kept on regular chow diet was collected and homogenized in BBL thioglycollate media and further processed in an anaerobic chamber with following gas mixture: 70% nitrogen, 20% carbon dioxide and 10% hydrogen. Ten-fold dilutions (10^6 and 10^7) of fecal content homogenate were cultured in a sterile 96-well plate in Brain Hearth Infusion broth (BHI), supplemented with 10% FBS and 0.5 g/l vitamin K3 (BHI-S) on 37°C for 2 days. *Prevotella*-positive wells were identified using *Prevotella*-specific 16S rRNA gene primers designed from preliminary metagenomic assemblies (see Key Resources Table). Positive wells were enriched in BHI-S medium containing vancomycin and BHI-S blood agar plates. Colonies were picked and streaked 3 times on agar plates before a pure culture was obtained. Isolates were confirmed by Sanger sequencing using the full 16S rRNA gene (primers 27F/1492R) and identified to known *Prevotella* spp. (blastn > 90% of similarity). Bacterial stocks were suspended in 25% of glycerol and cryopreserved at -80°C.

Mouse Strains

C57BL/6N mice used in this study were either purchased from different commercial vendors (SPF_jan, SPF_tac, SPF_chr, and SPF_env), or bred and maintained at the animal facilities of the Helmholtz Centre for Infection Research (HZI) (SPF_hzi, GF, SPF_nci, CONV_N6) (Table S1). SPF_nci and CONV_N6 mice were imported from Yale University and maintained under conventional housing conditions, while SPF_hzi mice were maintained at HZI under enhanced specific pathogen-free conditions (SPF_hzi). All mice were kept in individually ventilated cages (IVCs), and germ-free mice were bred and maintained in isolators (Getinge). All experiments were

performed with 8- to 12-week-old age-matched and gender-matched animals. Mice were fed *ad libitum* with a sterilized standard chow based on plant polysaccharides (Stand-PP) and were kept under a strict 12h light cycle.

All animal experiments were carried out in strict accordance with the German national and European laws and conformed to the Council Directive on the approximation of laws, regulations, and administrative provisions of the Member States regarding the protection of animals used for experimental and other scientific purposes (86/609/Eec). All animal experiments have been performed with the permission of the local government of Lower Saxony, Germany. Animal licence 33.19-42502-04-19/3267

METHOD DETAILS

In Vitro Polysaccharide Growth Assay

Prevotella spp. isolates were grown anaerobically in YCFA (Yeast extract, casitone, fatty acid) media until early exponential growth phase (OD600=~0.2). Cultures were passaged to pre-reduced YCFA + 0.5% (w/v) individual polysaccharides at a dilution of 1:100 in a total volume of 300 μl. Cultures were incubated anaerobically in multi-well plates at 37°C. Every hour, OD600 was measured using the Biotek plate reader after shaking the plate for 10s. OD was corrected for each polysaccharide condition by subtracting the average blank OD600 values from the raw OD600 values for each well. All cultures were grown in quadruplicates.

Total DNA Isolation and Whole Genome Sequencing

Total DNA was isolated from bacterial cells and stool pellets using a phenol-chloroform base protocol. Briefly for *Prevotella* isolates, cells were growth in 5ml BHI-S on 37°C (OD600 = 0.4). Then, cells were centrifuged 3,500 rpm and suspended with 500μl of extraction buffer (200 mM Tris, 20 mM EDTA, 200 mM NaCl, pH 8.0), 200 μl of 20% SDS, 500 μl of phenol:chloroform:isoamyl alcohol (24:24:1) and 100 μl of zirconia/silica beads (0.1 mm diameter). Bacterial cells/fecal pellets were homogenized with a bead beater (BioSpec) for 2 min. DNA was precipitated with absolute Isopropanol and finally washed with ethanol 70% vol. DNA extracts were suspended in TE Buffer with 100 μg/ml RNAse I and furthermore column purified. Total DNA was quantified and diluted to 25 ng/μl.

For Illumina library preparation, 60 μl of total DNA were used for sonication shearing (Covaris). Fragmentation was performed as follow: processing time = 150 s, Fragment size = 200 bp, Intensity = 5, duty cycle = 10. Illumina library preparation was perform using the NEBNext Ultra DNA library prep Kit (New England Biolabs inc.). The Library preparation was performed according to the manufacturer's instructions. We use as input a total of 500 ng of sheared DNA; the size selection was performed using AMPure XP beads (First bead selection = 55 μl, and second = 25 μl). Adaptor enrichment was performed using seven cycles of PCR using the NEBNext Multiplex oligos for Illumina (Set1 and Set2) (New England Biolabs inc).

Genome Assembly and Annotation

Short reads were obtained for each *Prevotella* species on the Illumina Hiseq 2500 2x100 bp. platform. The reads were assembled with SPAdes version v3.10.0 using "carefull" mode (Bankevich et al., 2012). Short contigs were then filtered by length and coverage (contigs > 500 bp and coverage > 5X). The obtained contigs were selected for scaffolding using SSPACE (Boetzer et al., 2011) version v2.0 and furthermore gene prediction and annotation was performed using PROKKA version v1.13.3 (Seemann, 2014) with default parameters.

16S rRNA Amplification and Sequencing

Amplification of the V4 region (F515/R806) of the 16S rRNA gene was performed according to previously described protocols (Caporaso et al., 2011). Briefly, for DNA-based amplicon sequencing 25 ng of DNA were used per PCR reaction (30 μl). The PCR conditions consisted of initial denaturation for 30 s at 98°C, followed by 25 cycles (10s at 98°C, 20 s at 55°C, and 20 s at 72°C DNA. Each sample was amplified in triplicates and subsequently pooled. After normalization PCR amplicons were sequenced on an Illumina MiSeq 2 x 250 bp platform.

16S rRNA Analysis

Obtained reads were assembled, quality controlled and clustered using Usearch8 version 8.1 software package (http://www.drive5.com/usearch/). Briefly, reads were merged using -fastq_mergepairs –with fastq_maxdiffs 30 and quality filtering was done with fastq_filter (-fastq_maxee 1), minimum read length 200 bp. The OTU clusters and representative sequences were determined using the UPARSE algorithm (Edgar, 2013), followed by taxonomy assignment using the Silva database v128 (Quast et al., 2013) and the Naïve Bayesian Classifier of the Ribosomal Database Project (RDP) (Wang et al., 2007) with a bootstrap confidence cut-off of 70%. OTUs phylogenetic inference was build using FastTree 2.1.3. (Price et al., 2010). The OTU absolute abundance table, mapping file and phylogenetic tree were used for statistical analyses and data visualization in R using the package phyloseq (McMurdie and Holmes, 2013).

Metagenomic Reconstruction of Mouse *Prevotella* MAGs

All Metagenome-assembled genomes (MAGs) belonging to the family Prevotellaceae were selected from the integrated Mouse Gut Metagenomic Catalog (iMGMC) (Lesker et al., 2020). In brief, the iMGMC comprehends 20,927 MAGs (quality MAG: completeness >= 50%, contamination < 10%) reconstructed by sample-wise and integrated assembly from 871 mouse gut metagenomic samples. For taxonomical identification, MAGs were clustered to 95% average nucleotide identity (ANI) using dRep (Olm et al., 2017) to 1,296

representative genomes. Taxonomic classification was performed using GTDBtk (reference database version r89) (Chaumeil et al., 2019). Classified representative MAGs were further used to identify the clusters of MAGs belonging to the family Prevotellaceae. A total set of 259 MAGs were retrieved and further used for genome-based phylogenetic analyses.

Phylogenetic Analyses

The phylogenomic analyses were conducted as previously described on the characterization of the *Prevotella copri* Complex (Tett et al., 2019) using the PhyloPhlAn version PhyloPhlAn2 v0.40 available in the "dev" branch of the repository (id b626e2dae732, https://bitbucket.org/nsegata/phylophlan). The phylogenetic analysis in Figure 1E was built using the 400 universal marker genes of the PhyloPhlAn database using the parameters ''–diversity low –fast''. The configuration file (config_file.cfg) was set with the following tools and parameters:

Diamond version v0.9.9.110 (Buchfink et al., 2015) with ''Blastx'' for the nucleotide-based mapping, ''Blastp'' for the amino-acid based mapping, and ''–more-sensitive –id 50 –max-hsps 35 -k 0'' in both cases.

MAFFT version v7.310 (Katoh and Standley, 2013), with ''–localpair –maxiterate 1000 –anysymbol –auto'' options.

trimAl version 1.2rev59 (Capella-Gutiérrez et al., 2009), with ''-gappyout'' option.

IQ-TREE multicore version v1.6.9 (Nguyen et al., 2015), with ''-nt AUTO -m LG'' options.

RAxML version 8.1.15 (Stamatakis, 2014), with ''-p 1989 -m GTRCAT -t'' options.

The phylogeny in Figure S5C was built with PhyloPhlAn with the same options as reported above. The phylogenies of *SusC* and *SusD* in Figures 6C and 6D were performed using the amino acid sequences of all predicted *SusC/D* genes occurring into PULs of the mouse *Prevotella* genomes and the reconstructed *P. corpi* MAGs from Italy (De Filippis et al., 2019). *Bacteroides ovatus* strain ATCC 8483 arabinoxylan SusC/D (BACOV_03426: BACOV_03429) and (BACOV_04392: BACOV_04393) were included as references. Sequences were aligned with MAFFT (–maxiterate 1000 –retree 1 –localpair) and phylogenetic inference was performed using RAxML-HPC-PTHREADS-SSE3 version 8.2.10 (-f a -m PROTGAMMAVT -p 12345 -x 12345 -# 1000) with 1000 bootstrap replicates. The phylogenetic trees in Figures 1, 6C, 6D, and S5 were visualized in R using the package ggtree_v2.0.0 (Yu et al., 2018).

Automated Reconstruction of *P. copri* MAGs

In this study we reanalyzed and expand the metagenomic analysis of a recent dataset dominated by *Prevotella* spp. (De Filippis et al., 2019). This study performed deep sequencing of the gut microbiome of 101 healthy Italian individuals with distinct diets and lifestyles (Omnivore, n = 25; Vegetarian, n = 39; Vegan, n = 37) distributed in two sequencing projects (NCBI SRA: SRP126540 and SRP083099). Sample-wise assembly, annotation, and integrative genomic binning was performed with ATLAS metagenomic workflow (Kieser et al., 2019) using the version 2.1.3 (commit a007857, https://github.com/metagenome-atlas/atlas). The default configuration file was set with the following parameters: ''assembler: spades'', ''Binning: DASTool'', genome dereplication ''ANI: 0.95, completeness: 50, contamination: 10''. Taxonomical assignment was performed with the CAT database (von Meijenfeldt et al., 2019). Genome abundance estimates were calculated for each sample in the dataset by mapping the reads to the non-redundant MAGs using BBmap and determining the median coverage across each of the MAGs.

PUL Analysis in *Prevotella* Genomes and MAGs

Identification of Carbohydrate-Active Enzymes (CAZymes) was performed using dbCAN2 (Zhang et al., 2018) version v2.0.6 (CAZy-DB= 07312019, https://github.com/linnabrown/run_dbcan). The results were filtered by the number of tools that identified a CAZyme protein ''#ofTools >= 2'', and the family-domain assignments were defined based on the HMM database. Polysaccharide utilization loci (PUL) and *susC/D* gene annotations were performed using PULpy (Stewart et al., 2018) (commit 8955cdb, https://github.com/WatsonLab/PULpy) using a sliding window of five genes and an intergenic distance 500 bp. The tool was implemented with the updated CAZy-DB-07312019 from dbCAN2. Prediction of the PUL's metabolic function was performed based on the enriched CAZymes within each PUL and its linked trophic guild (Tables S3 and S4) (Accetto and Avguštin, 2015). Predicted PULs were visualized in R using the package *gggenes* v0.4.0.

Total RNA Isolation and RNA-seq Library Preparation

High quality RNA was isolated using acid-phenol chloroform-based protocol (Ridaura et al., 2013). Briefly for *in vitro* treatment, bacterial cells were grown in BHI-S on 37°C to an OD600 = 0.4). For *in vivo* sampling, intestinal content (~100 mg) was immediately preserved using bacterial RNA-protect (QIAGEN) and cryopreservation (-80°C). Cell disruption was done using a fastprep (MP) in presence of 200 μL of zirconia beads (0.1 μm diameter) and lysis buffer (200 mM NaCl, 20 mM EDTA), 220 μL of 20% SDS, 600 μL of phenol:chloroform:isoamyl alcohol (pH 4.5, 125:24:1, Ambion). After centrifugation (12,600 rpm x 5 min at 4°C), the supernatant was discarded and the dry pellets were used for RNA purification with an equal volume of acidic phenol chloroform. The total RNA was precipitated using 2 volumes of Isopropanol (>3 hours of incubation) and centrifugation for 30 min 12,600 x rpm at 4°C. RNA pellets were washed with 750 μl of cold EtOH 75% and suspended in 90 μl of 1x TE. DNase treatment was done with 2 units of TURBO DNase (Ambion) and furthermore the reaction was purified in silica-based columns using the RNeasy Kit (Qiagen).

For library preparation, RNA quality was evaluated using bioanalyzer nano-chip (Agilent technologies), samples were selected according to RNA integrity score (RIN > 8.0). Due to the gut microbiota samples contain a high amount of host and bacteria rRNA, we used the Ribo-Zero Gold Epidemiology (Illumina, CA. USA), After rRNA depletion, the mRNA was fragmented to 200 bp by sonication (Covaris, processing time = 150 s, Fragment size = 200 bp, Intensity = 5, duty cycle = 10) and evaluated again for quality and size. For

each sample a total of 100 ng of fragmented mRNA was used as an input for cDNA synthesis and Illumina sequencing adaptor ligation. Illumina sequencing libraries were prepared using a directional RNA Library kit (NEBNext Ultra) (New England Biolabs inc) following manufactures' protocol.

Differential Gene Expression RNA-seq Analysis

Reads were quality filtered using Trimmomatic (Bolger et al., 2014) version v0.33 with as follow parameters (LEADING:3 TRAILING:3 SLIDINGWINDOW:4:15 MINLEN:35 HEADCROP:3). After quality control reads were aligned to each mouse *Prevotella* reference genome using STAR (Dobin et al., 2013) version v2.5.2a. Reads count was performed using HTseq (Anders et al., 2015) version v0.11.2. Normalization and differential expression were quantified in R using the DEseq2 package (Love et al., 2014) version v1.26.0. The code implemented in the analysis is available as supplemental R notebooks and data is accessible at (https://github.com/strowig-lab/galvez_et_al_2020/)

Microbiota Manipulation and Diet Interventions

For every experiment, *P. Intestinalis*, *P. rodentium* or *P. muris* cultures were freshly grown anaerobically in BHI-S medium on 37°C, and SPF_hzi mice were colonized by oral gavage, with each bacterium at a dose $3x10^8$ CFU suspended in 200 μl of BHI medium. For *Prevotella* isolate competition experiments, mice were colonized with an equivalent mixture of bacteria by mixing single bacterial cultures in a 1:1 ratio (each $1x10^8$ CFU suspended in 200 μl BHI medium). Fecal microbiota transplantation (FMT) experiments were performed as previously described (Thiemann et al., 2017). In brief, fecal content of donor mice (CONV_N6 and SPF_jan) was collected, transferred to BBL thioglycollate media and weighed. Under anaerobic conditions, fecal content was homogenized, filtered through a 70 μm cell strainer, and diluted to a concentration of 40 mg/ml. After centrifugation (10 min, 500 g, 4°C), fecal material from each donor was resuspended in BHI medium and mixed in 1:1 ratio. A total of 200 μL of mixed fecal transplant was given by oral gavage to recipient mice. Before and after colonization, fecal samples were collected on different days and *Prevotella* spp. colonization kinetics was examined by 16S rRNA sequencing.

For performing diet intervention experiments, mice on Stand-PP were colonized two weeks in advance by receiving a single gavage of 200 μl of BHI-S containing *P. intestinalis* alone, or a mixture of equal amounts of *P. intestinalis* and *P. rodentium*. A following diet intervention for 7 days was performed with semisynthetic diet sterilized by gamma irradiation. The used diet in this experiment were Synth-HF, a high-fat diet (45kJ% fat, lard, SSNIFF D12451) and Synth-LF, a diet low in fat and high in sugar (10kJ% fat, 33% sucrose, SSNIFF D12450B). Mice receiving an additional polysaccharide supplementation were provided with autoclaved drinking water ± 1% (w/v) of individual polysaccharide.

QUANTIFICATION AND STATISTICAL ANALYSIS

Statistical Analysis

Statistical analyses were carried out in R (R Core Team, 2019) and figures were produced using the package ggplot2 (Wickham, 2016). Principal Coordinates Analysis and Non-Multidimensional scaling NMDS was carried out on a distance matrix calculated on Bray Curtis's distance (package vegan and phyloseq). Multivariate Analysis of Variance (adonis function in package vegan) was carried out on Bray Curtis' dissimilarity matrix to identified the variation explained (R^2) on the tested variables. Pair-wise Wilcoxon-Mann-Whitney and Kruskal-Wallis test was used to test differences in Carbohydrate-active Enzymes (CAZymes) and relative abundance of *Prevotella* spp with *p*-adjusted values (*p-adj*) using the Benjamini–Hochberg method for multiple comparisons. Differences in alpha diversity were statistically significant as determined by Tukey's 'Honest Significant Difference' method with *p*-adjusted values (*p-adj*) for multiple comparisons. Quantification of the bacterial growth *in vitro* was quantified in R.

The *p-value* < 0.05 was considered statistically significant (*p-value* < 0.001***, 0.01**, 0.05*). All computational and statistical analyses were performed using open-source software as described in the main text and STAR Methods.

The exact values of n (number of samples or individuals) for each experiment are listed in the figure legends, and the definitions of center, variance, statistical test and *p*values are presented in the figures when visualization is allowed or in the figure legend respectively.